SAND2018-11861PE

Shale Science & Gas Well Production Enhancement

Hongkyu Yoon

Geomechanics Department

Sandia National Laboratories

Exceptional service in the national interest

SAND2018-XXXX

Sandia National Laboratories is a multimission laboratory managed and operated by National Technology and Engineering Solutions of Sandia, LLC, a wholly owned subsidiary of Honeywell International, Inc., for the U.S. Department of Energy's National Nuclear Security Administration under contract DE-NA-0003525.

Acknowledgments

- Laboratory Directed Research and Development program at Sandia National Laboratories

- U.S. Department of Energy Office of Basic Energy Sciences, Division of Chemical Sciences, Geosciences, and Biosciences

- Thomas Dewers, Mathew Ingraham, Bill Mook (SNL)
- R. Charles Choens, Kyung Won Chang, Byoung Yoon Park (SNL)
- Peter Mozley, Oh-Tark Kwon (NMT, KOGAS)

SANDIA NATIONAL LABORATORIES OVERVIEW

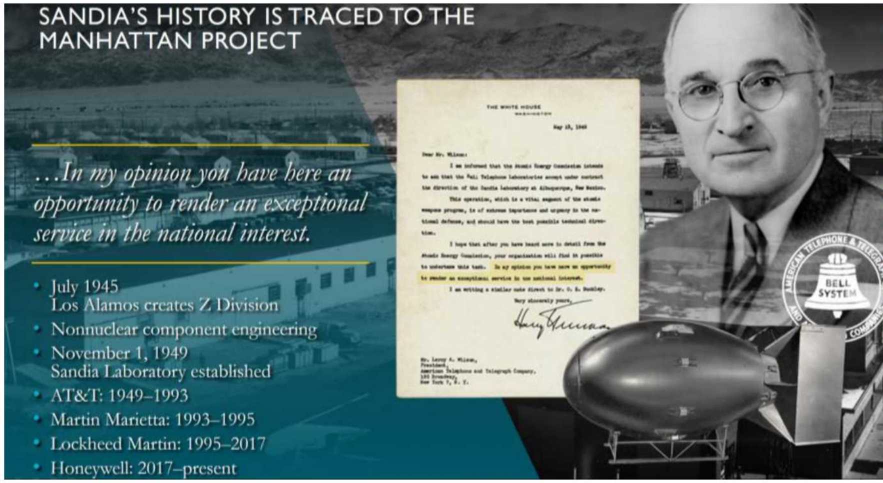

SANDIA ADDRESSES NATIONAL SECURITY CHALLENGES

SANDIA'S BUDGET and WORKFORCE

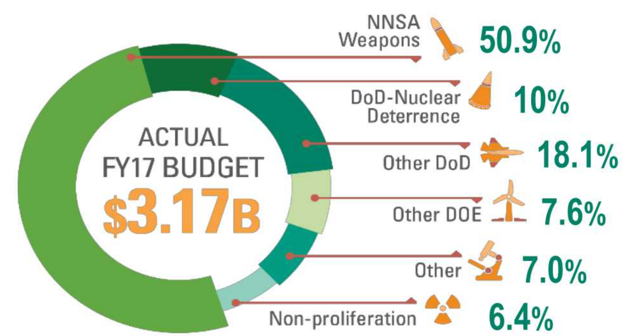

~12,300 EMPLOYEES

~11K New Mexico

~1.3K California

2017

Subsurface Energy Activities

- Subsurface energy technologies typically involve the change of fluid flow, stress, thermal, chemical (aka THMC) status in fractured and porous media
  - Unconventional resources recovery
  - Disposal of wastewater and nuclear waste
  - Subsurface carbon and compressed gas storage
- To improve modern energy activities and reduce adverse risks (e.g., induced seismicity and environmental impact), current understanding of poromechanics, averaging conceptual models (e.g., cubic law and biot effective stress), and coupled effects on flow paths needs to be improved
- Mesoscale analysis – linking discrete and complex pore-scale behavior to continuum (macroscale) reservoir response – is key, yet remains elusive as a result of the extreme heterogeneity and resulting scale dependence.

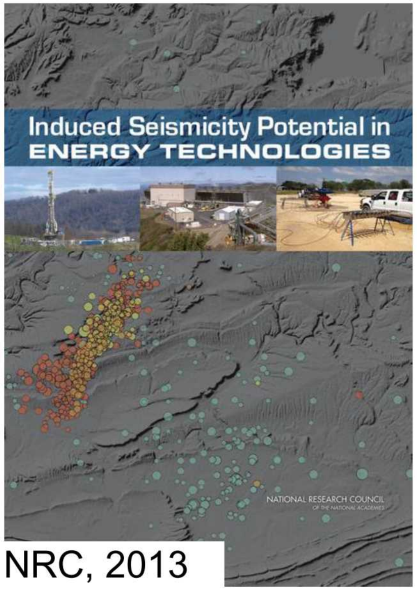

NRC, 2013

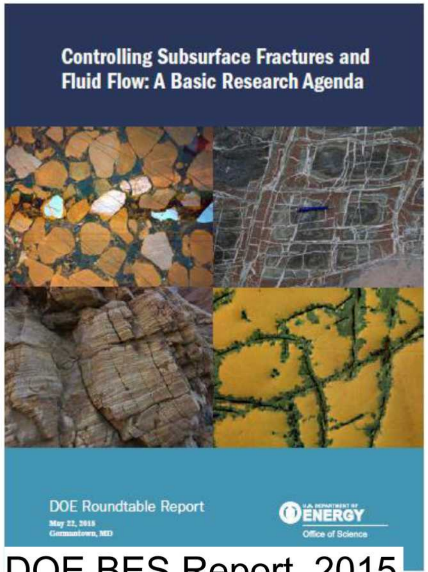

DOE BES Report, 2015

Multiscale Heterogeneity in Compositions, Pore structure, and Mechanical Properties

► Understand how heterogeneity, pores, cracks, flaws etc. contribute to shale poromechanics over scales and provide physical basis for core-scale measured deformational and transport constitutive behavior

► Develop novel techniques and workflow for a linked imaging, experimental, and modeling-based advancement of shale poromechanics

Quartz area, 20 indents
Load-displacement

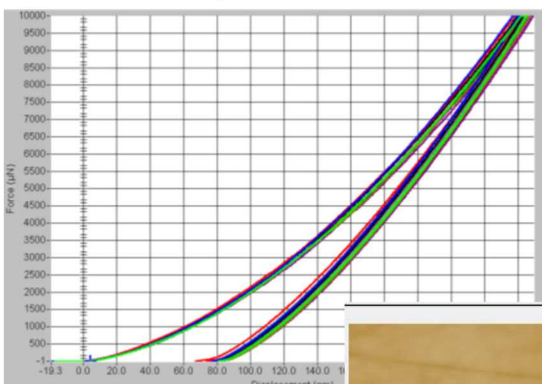

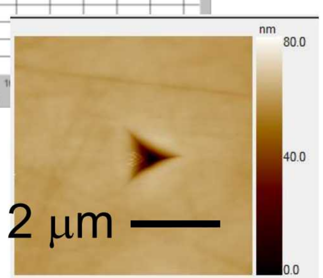

Er (Gpa) =
80.8 ± 1.3

Clay-rich area, 64 indents
Load-displacement

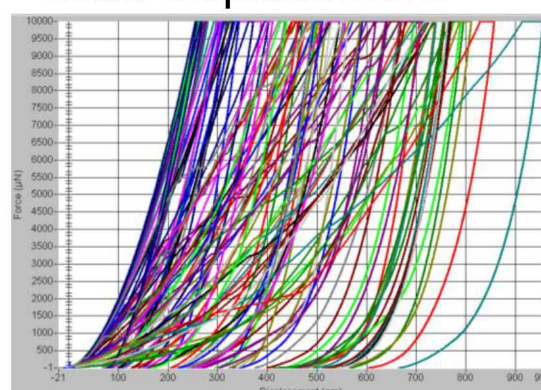

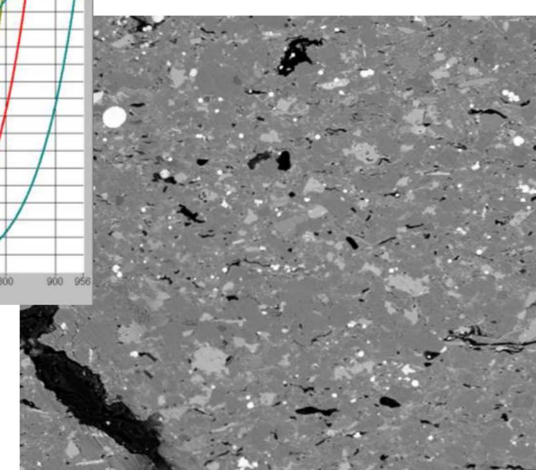

Multiscale characterization of physical, chemical, and mechanical heterogeneity of nano-porous geomaterials

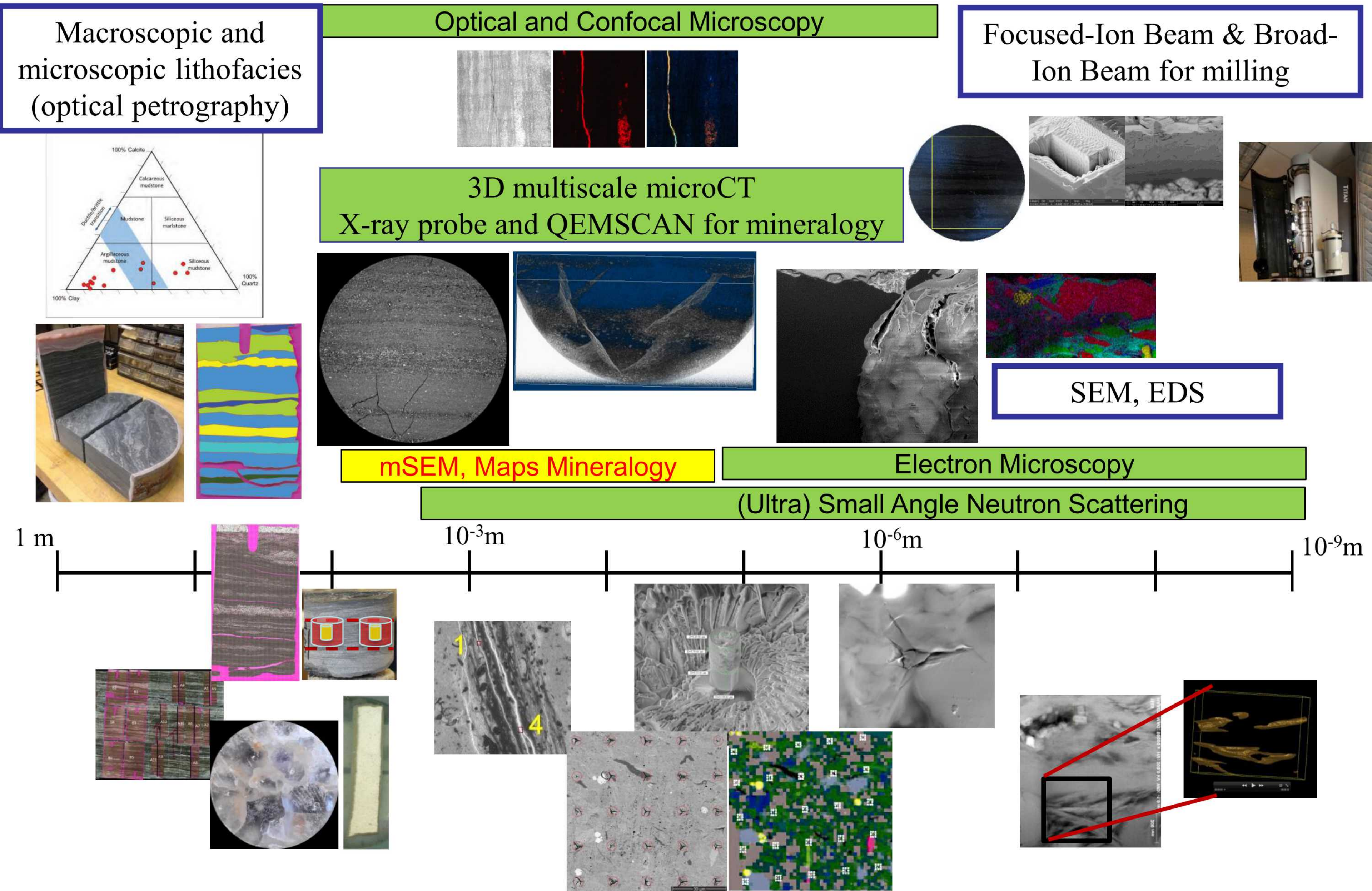

Approach

- **40 cm diameter core of Mancos Shale**
  - Interlaminated fine mud, medium/ coarse mud, and very fine sand
  - 1-3 mm laminae
  - Parallel lamina, wavy lenticular lamina, ripple forms, and bioturbation
- **Mineralogical and textural characterization**
  - Macroscopic
  - Optical petrography/microscopy
  - Micro-CT
  - FIB-SEM
  - BSE
  - MAPS Mineralogy
- **Mechanical tests**
  - Uni-/Tri-axial compression (1x2”)
  - Brazilian Test (1x0.5”)
  - Nanoindentation
- **Computational modeling**

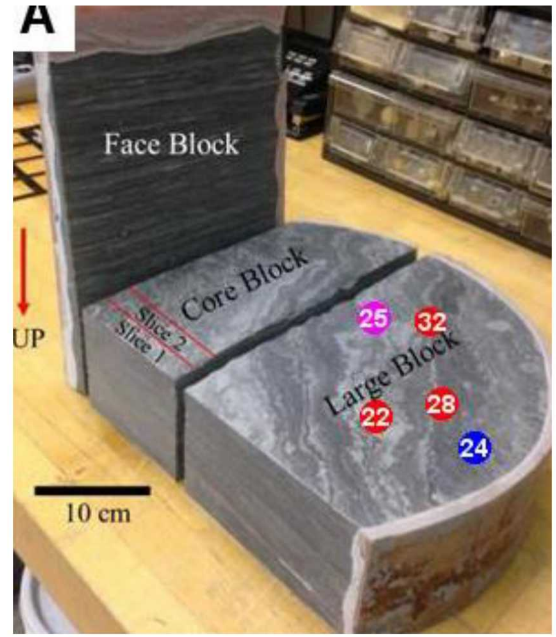

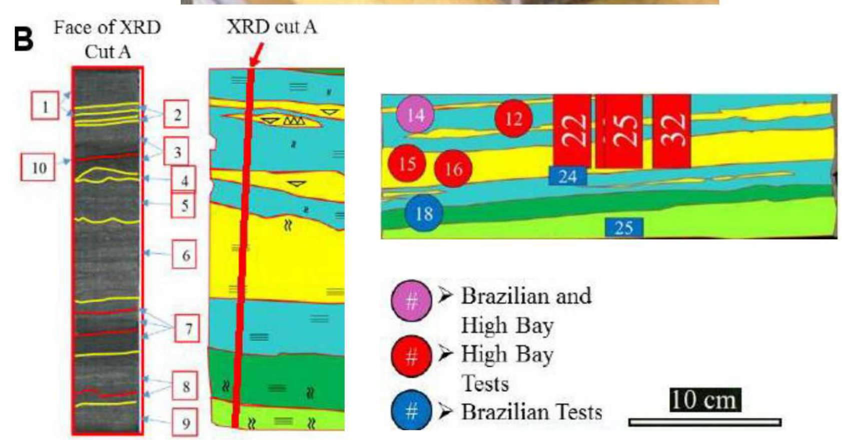

Yoon et al. (AAPG, Memoir 2019, in press)
Dewers et al. (AGU, Monograph, 2019, in press)

MAPS Mineralogy

- **SEM-based automated mineralogical measurement, analysis, data integration**
  - – Collection, overlay and re-registration of multiple images from different modalities
  - – SEM, SEM-EDS, optical, CL, EBSD
  - – QEMSCAN measurement algorithms
- **Mineral identification**
  - – Spectral matching
  - – Each pixel – single/multiple minerals
  - – Elemental substitutions
  - – Simultaneous mineral element and count maps

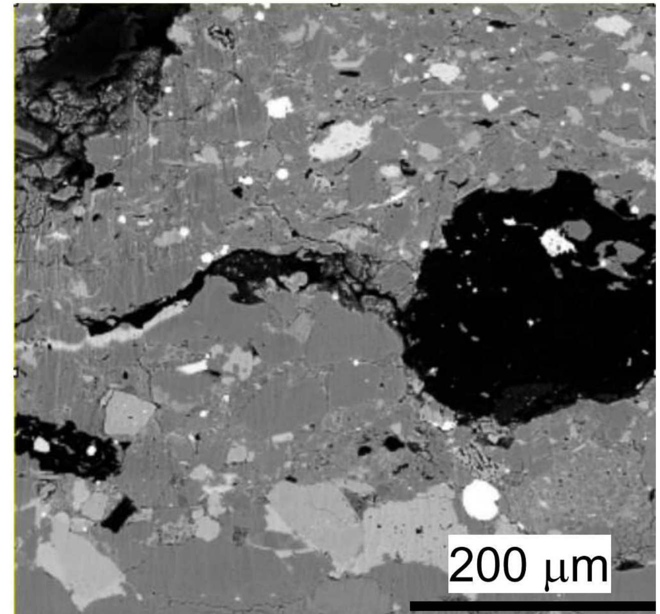

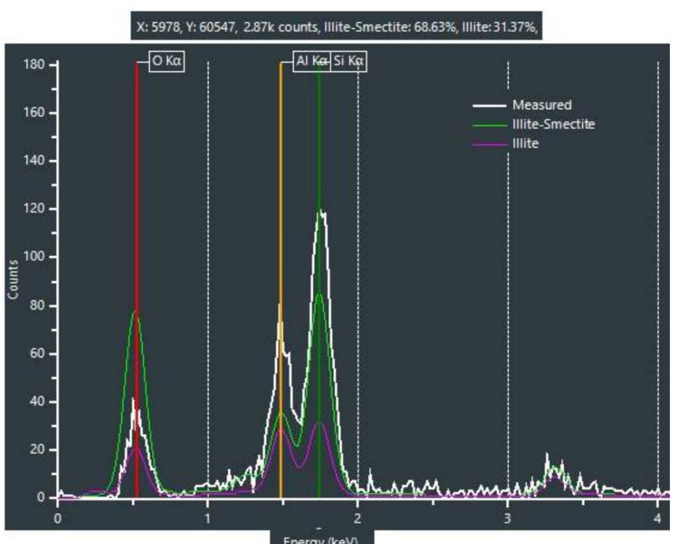

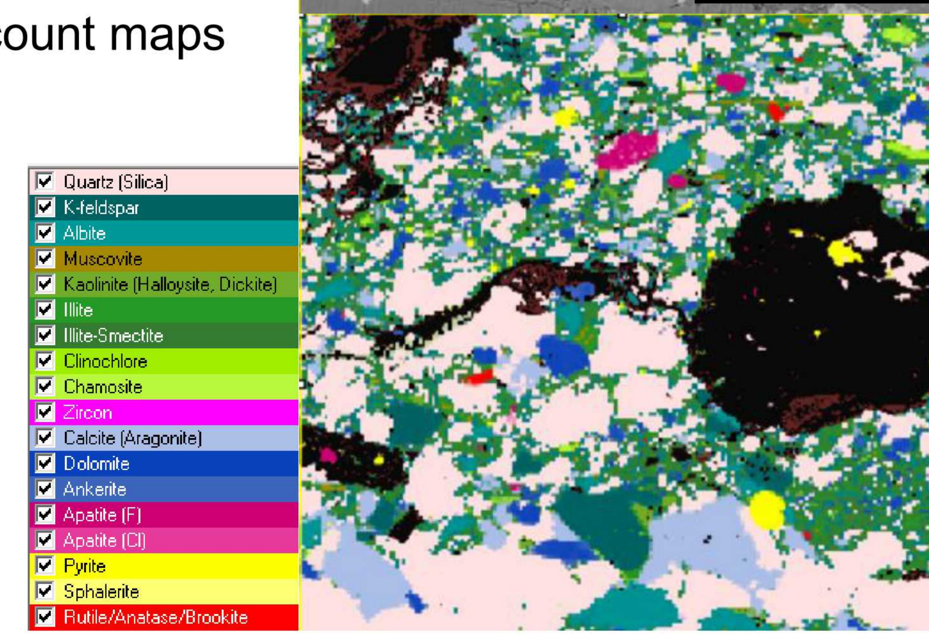

Mineralogy Mapping

Ion-milling polished Mancos
(1 inch diameter)

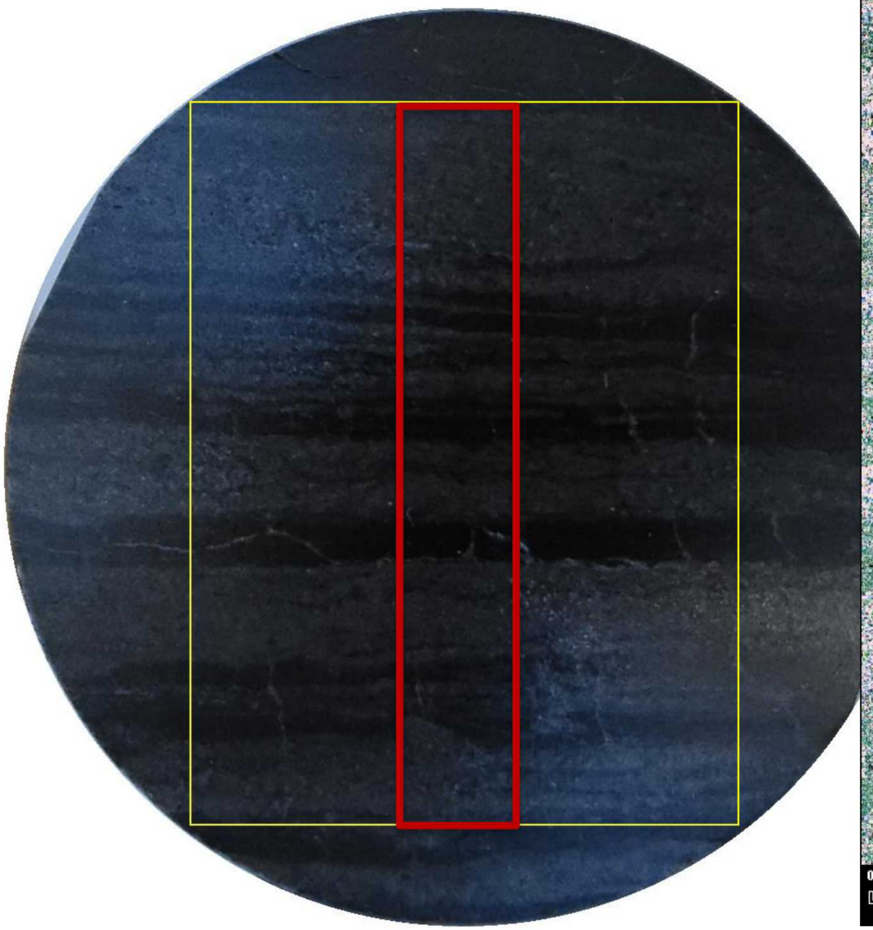

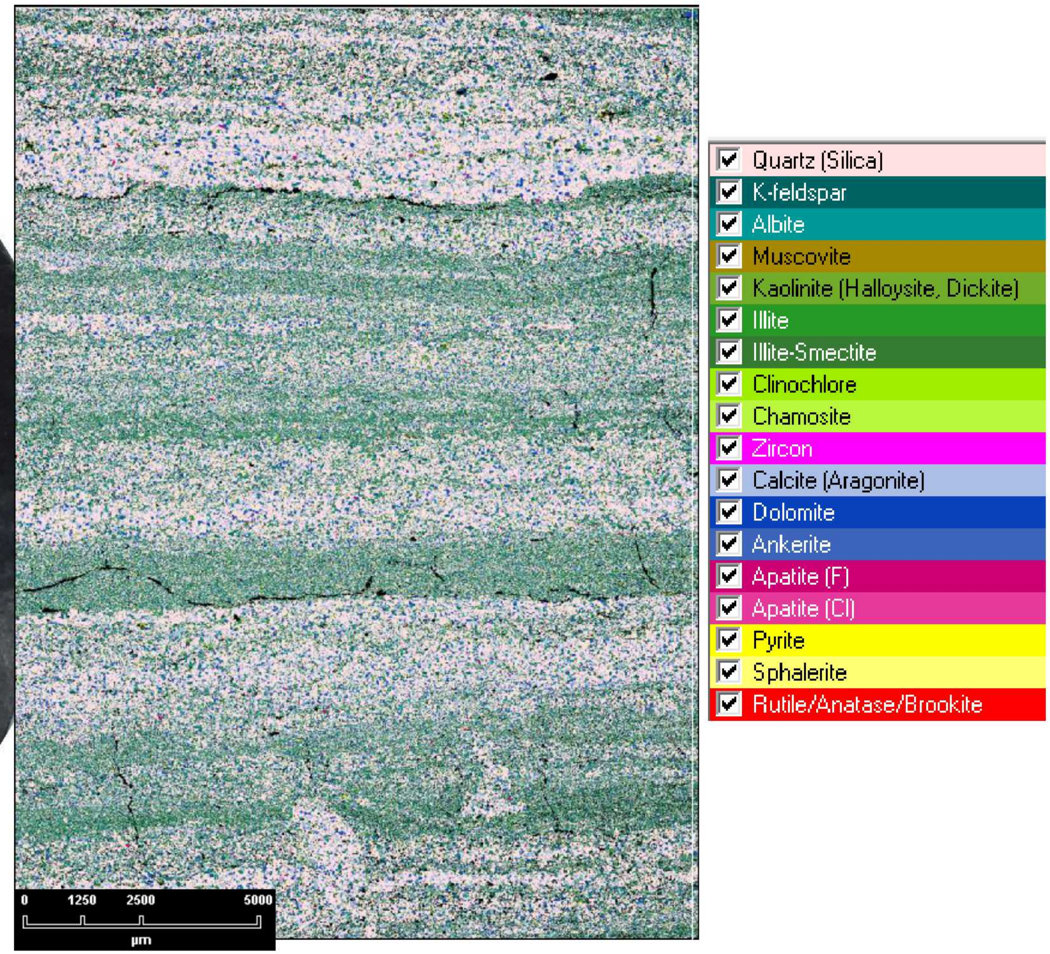

Yellow Box (1.45 x 1.98 cm): BSE @ 1µm & MAPS @ 10µm
Red box (0.18 x 1.98 cm): BSE @ 0.2µm & MAPS @ 2µm

Mineralogy Mapping: Scale/methods dependent

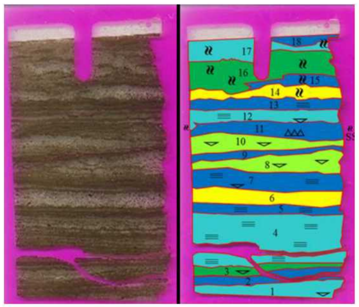

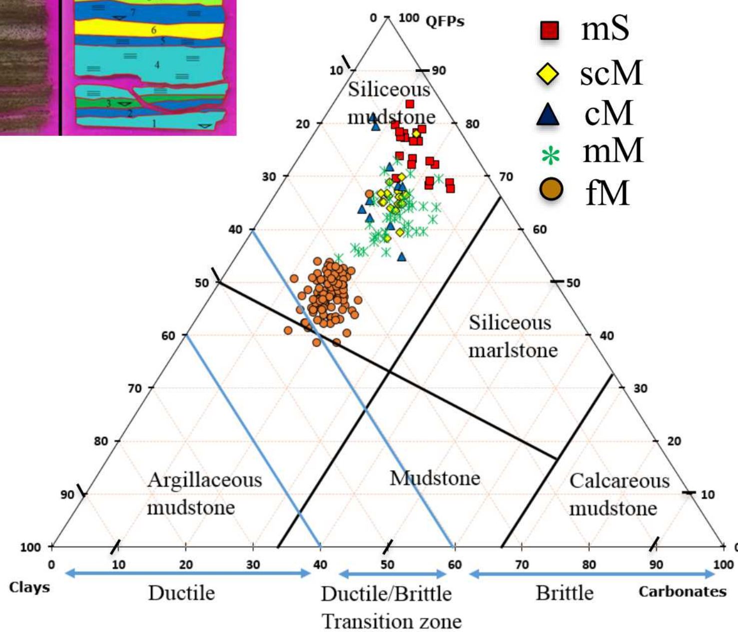

MAPS

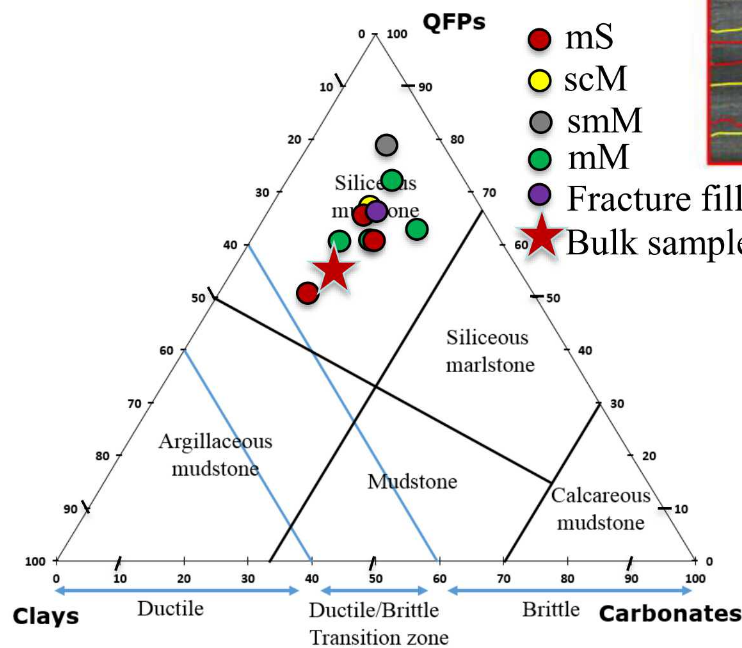

XRD

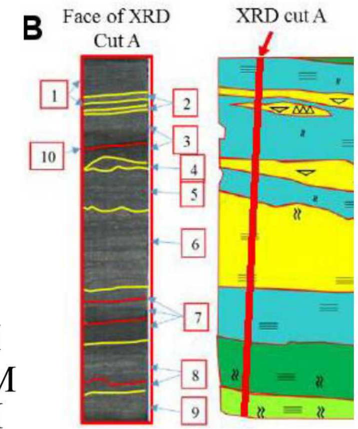

Yoon et al. (AAPG, Memoir 2019, in press)

Mineralogy Mapping: Scale/methods dependent

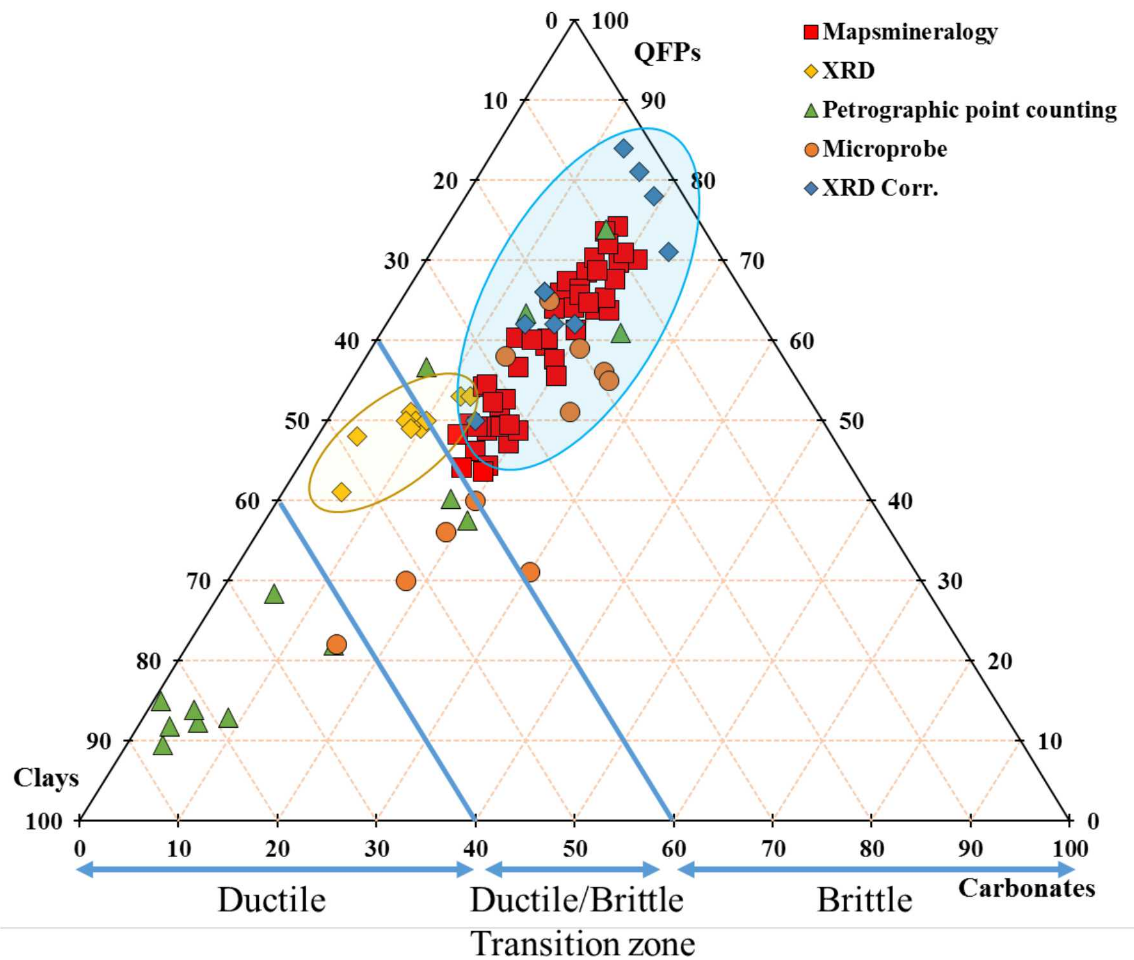

Kwon (@NMT, MS work, 2018)

Influence of geological attributes on mechanical properties

Micro-lithofacies

mS

scM

cM

mM

fM

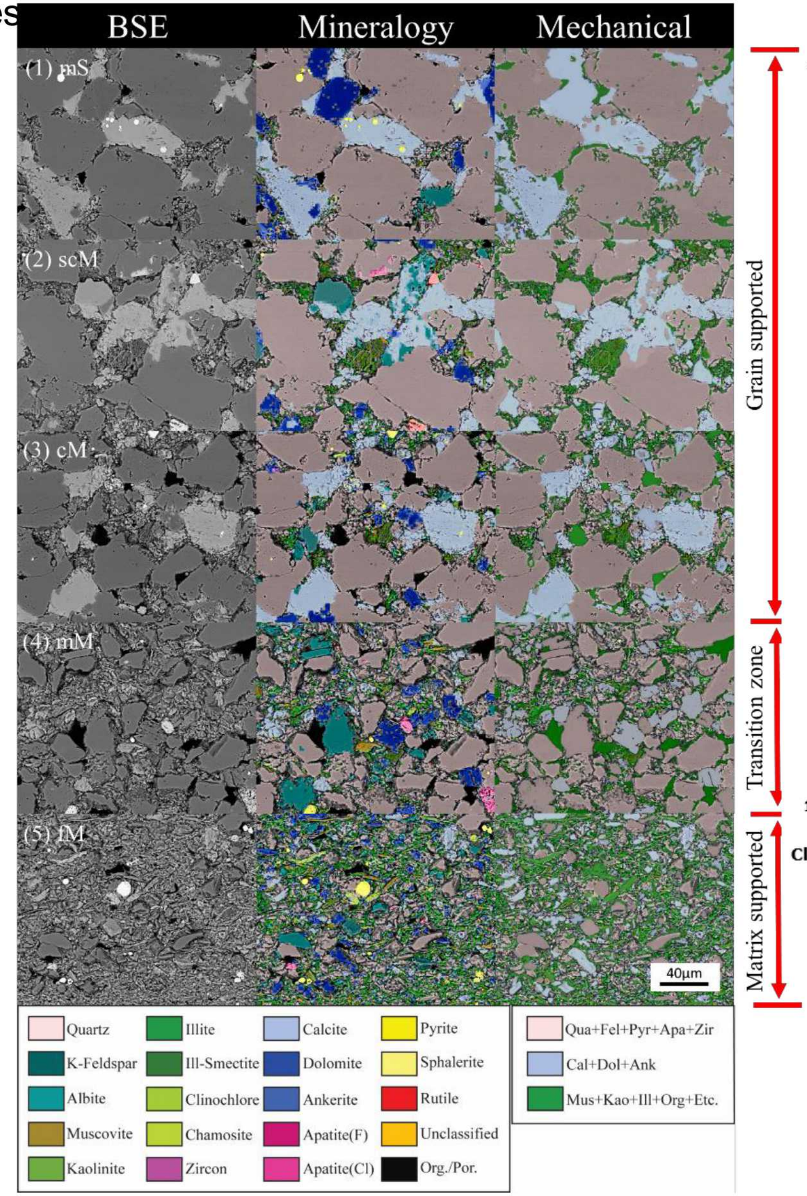

Mineral Assemblages

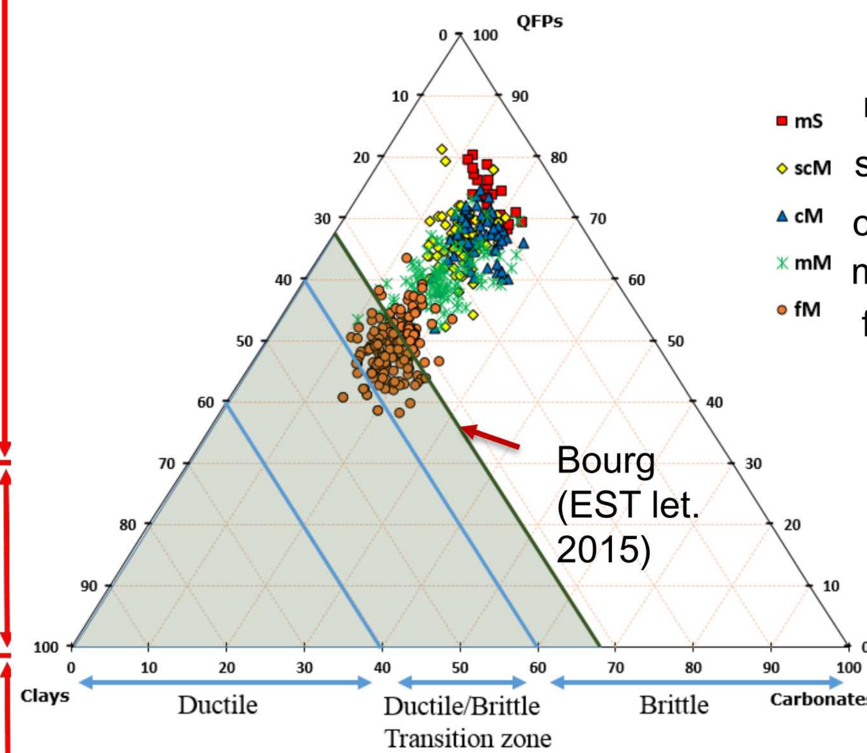

mS
scM
cM
mM
fM

Ulmer-Scholle et al. (2014)

Kwon (@NMT, MS work, 2018)

Conceptual Model of Anisotropic Layered System

QFPs
Carbonate

Clay
Organics

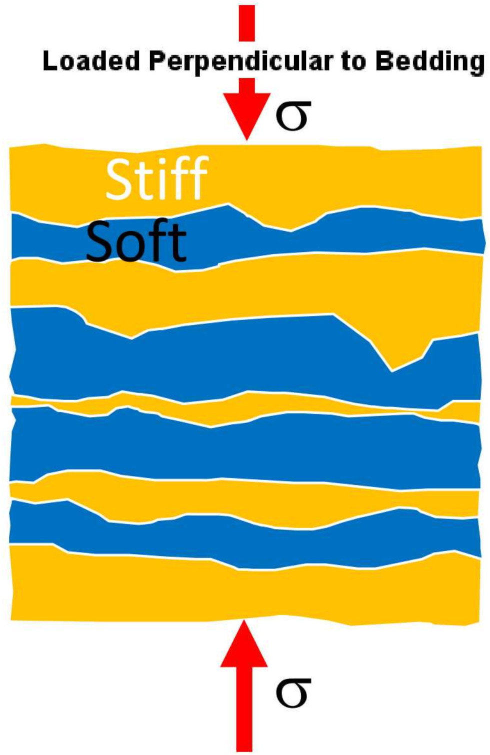

$\sigma_{stiff} = \sigma_{soft} = \sigma$

$\varepsilon_{stiff} < \varepsilon < \varepsilon_{soft}$

Overall strain

>

P wave velocity

<

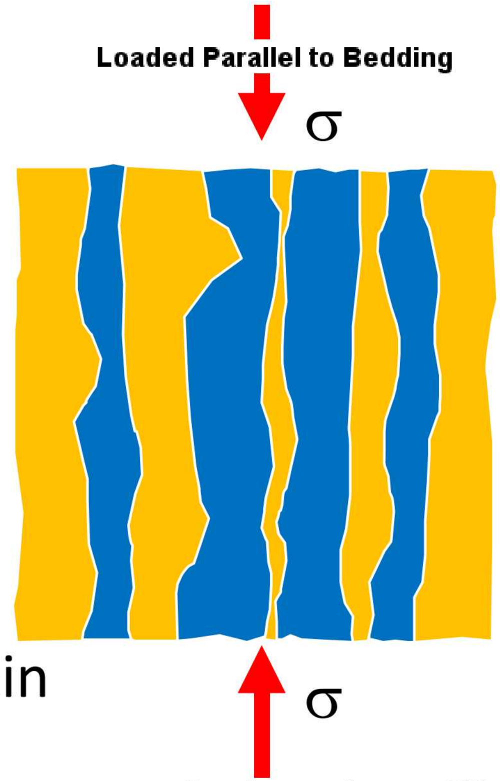

$\sigma_{soft} < \sigma < \sigma_{stiff}$

$\varepsilon_{stiff} = \varepsilon = \varepsilon_{soft}$

Axisymmetric Compression Testing

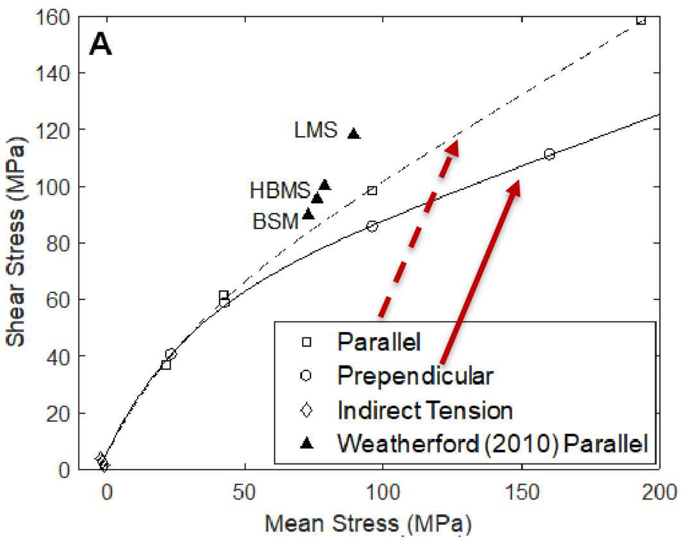

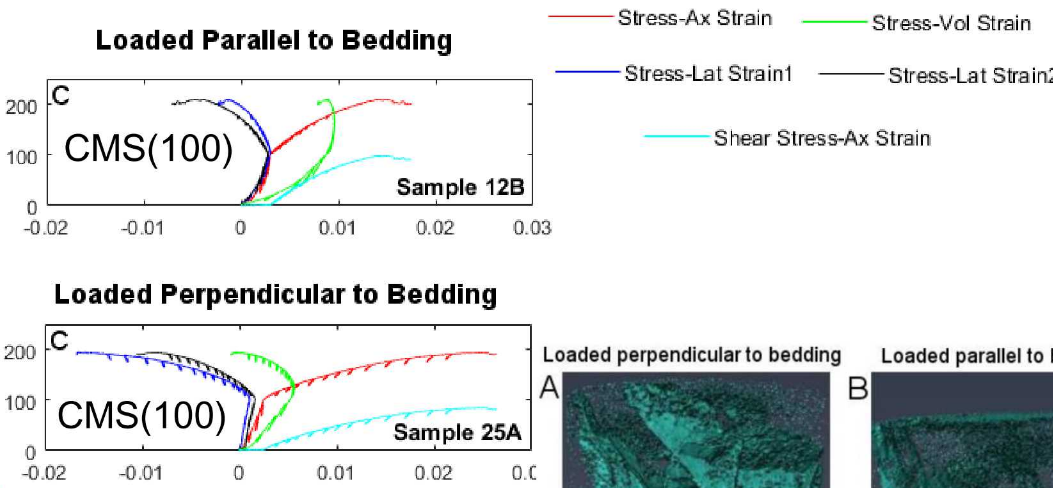

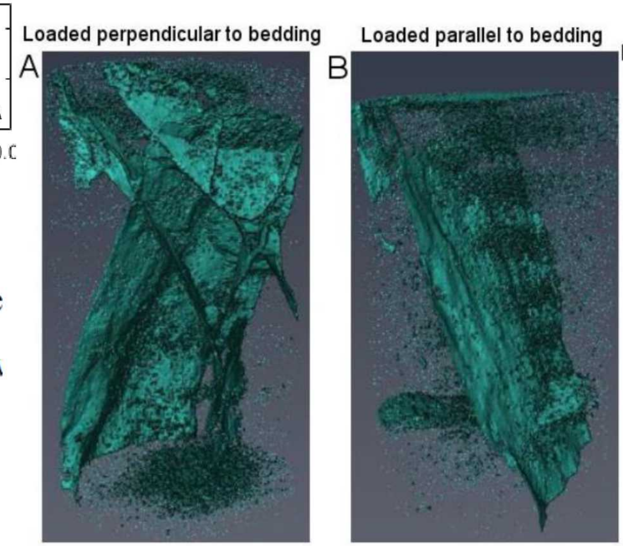

Segmented MicroCT images

	Confined (MPa)		Axial Stress	Mean Stress	Shear Stress	Fracture Angle (
15B	CMS (50)	Parallel	113.00	42.20	61.31	13.5
28A	CMS (50)	Perpendicular	110.64	42.80	58.75	15.5
12B	CMS (100)	Parallel	209.59	96.09	98.30	23.5
25A	CMS (100)	Perpendicular	195.07	96.20	85.62	30
14B	CMS (200)	Parallel	376.37	193.42	158.44	27.5
22A	CMS (160)	Perpendicular	288.64	160.31	111.14	35.5

CMS: Constant Mean Stress

Yoon et al. (AAPG, Memoir 2019, in press)

Axisymmetric Compression Testing

Horizontal slice through the central part of sample

One primary & two secondary fractures

A. Loaded parallel to bedding (15B)

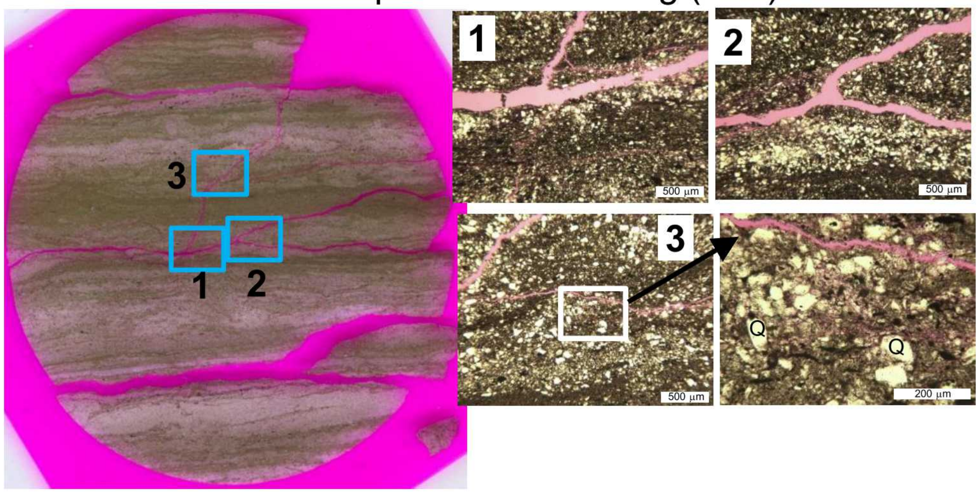

Fracture intersection & bifurcation with small aperture microfractures

Microfracture propagation in between quartz grains

Curved main fracture

B. Loaded perpendicular to bedding (28A)

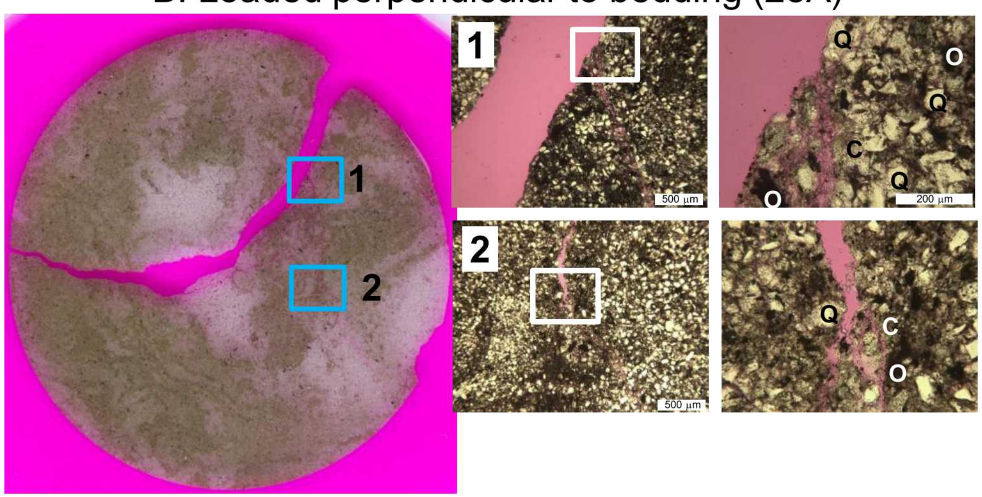

Microfracture patterns in between quartz grains

Indirect Tension Results

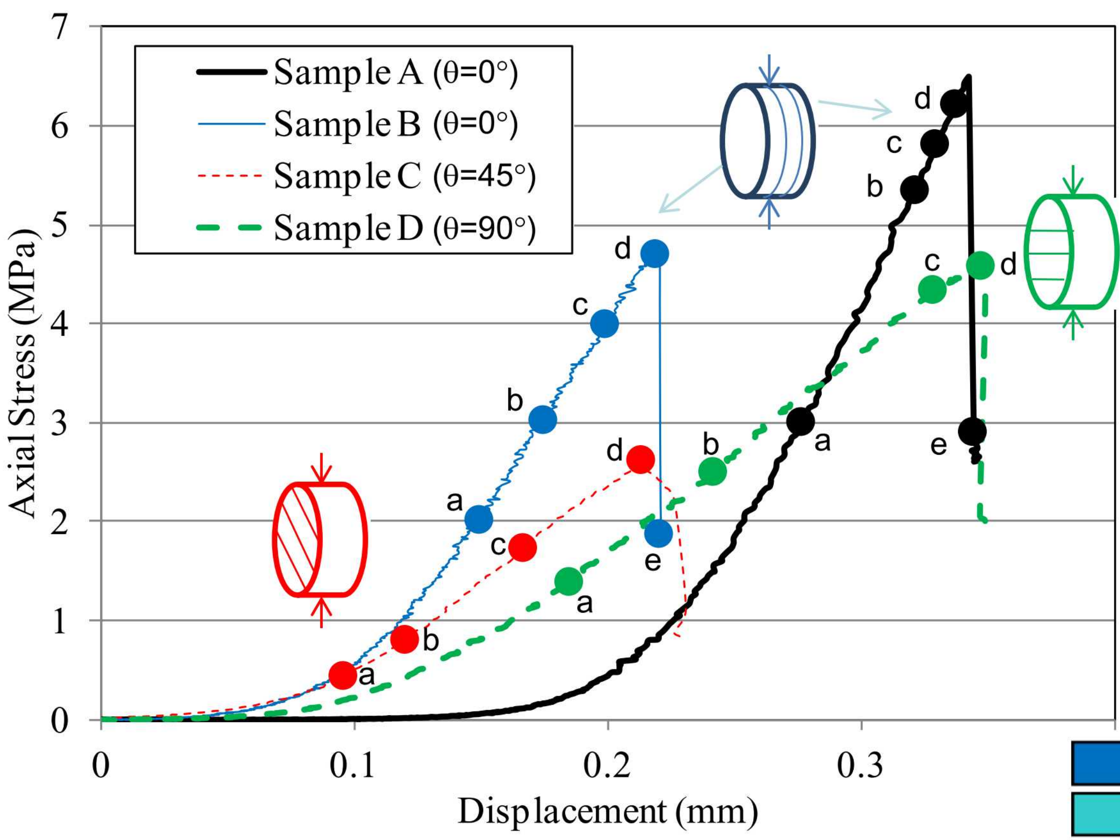

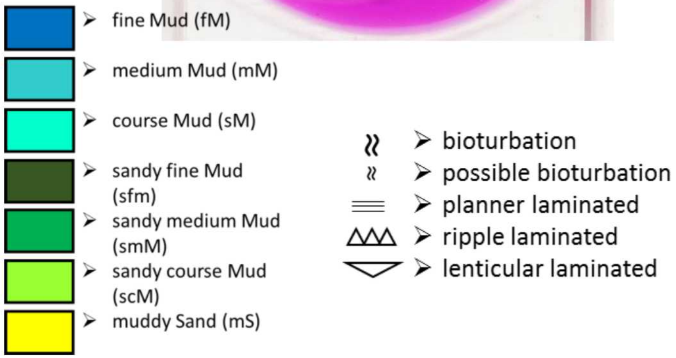

$$\sigma_t = \frac{2P}{\pi D t}$$

P: Loading

D: Diameter

t: thickness

Na et al. (JGR 2017)

Tensile Strain Distribution (Digital Image Correlation)

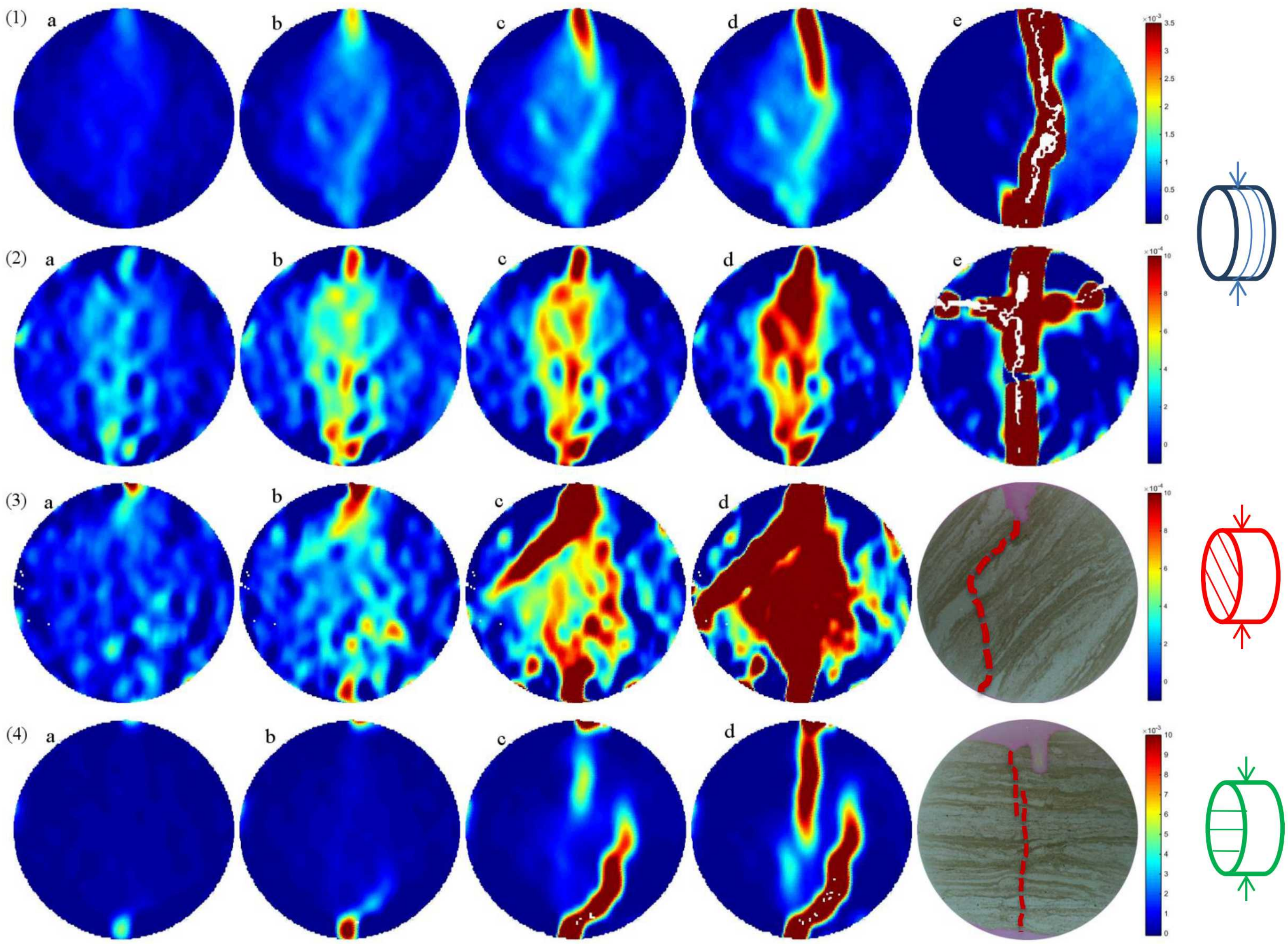

Numerical Simulations of Brittle Fracturing

- Phase field model for crack representation (Heister et al,2015)
- Shale is modeled as two-constituent brittle materials with stiff and soft layers:
  - Young's Modulus
  - (Pore pressure)
  - (Chemo-mechanical coupling)

Crack phase field (φ)

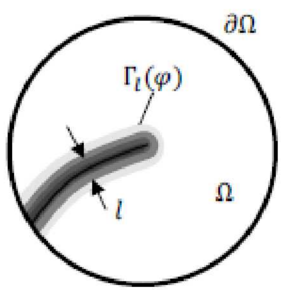

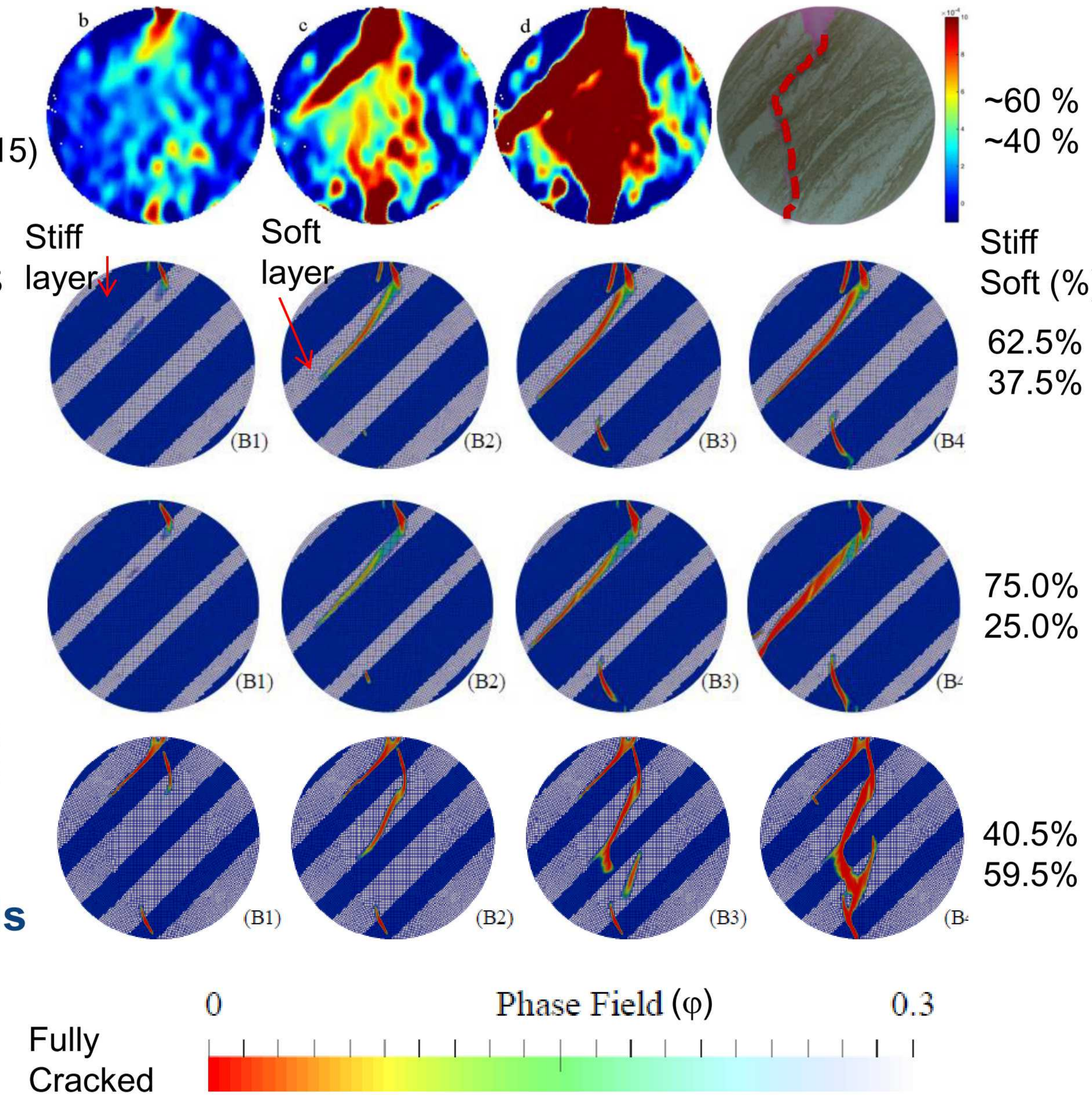

Differential Equations Analysis Library.II (Bangerth et al., 2007; 2013)

DEAL.II Open Source Finite Element Library

Effective Properties of Heterogeneous Materials

- Transversely isotropic effective medium for elastic parameters (Berryman, 1998)
  - Spatial homogenization procedure leads to much simpler crack patterns than those from the layered isotropic materials
  - Crack paths in the effective medium are less tortuous due to (probably) filtering out mesoscopic information via homogenization
  - Smaller surface area created by the fracture process yields the reduced tortuous crack paths with a diminished amount of energy dissipation (much higher effective fracture toughness)

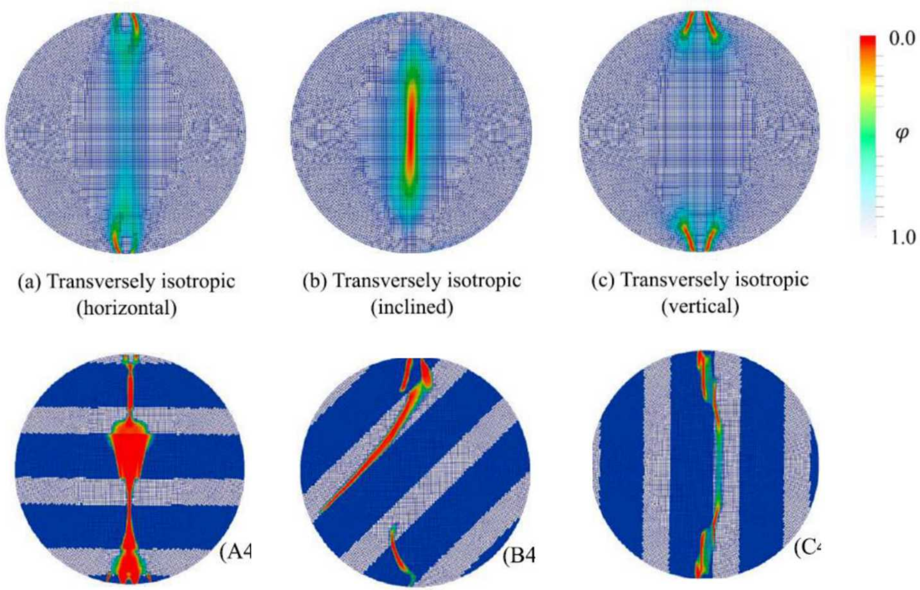

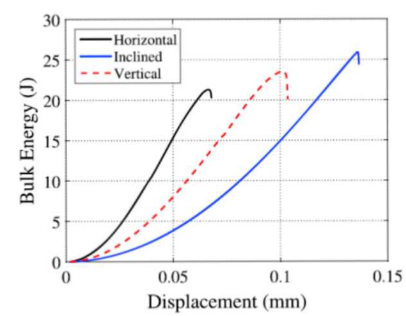

Transversely Isotropic

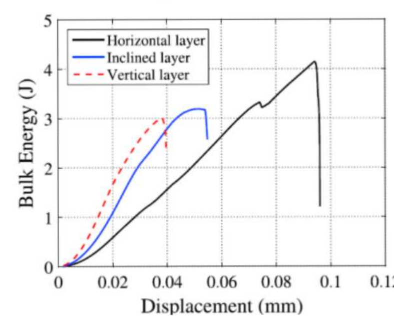

Layered Isotropic

Na et al. (JGR 2017)

NanoIndentation

- **Depth sensing/instrumented indentation**
  - – highly accurate load-displacement record
  - – Analytical models to determine modulus, hardness and other mechanical properties using the load-displacement data

- **Analytical concept**
  - – Purely elastic deformation upon initial unloading
  - – Contact between a rigid indenter and homogeneous isotropic elastic half spacing
  - – Compliance of the sample and indenter tip – springs in series
  - – Hardness = load/contact area
  - – Elastic modulus determined by stiffness (S)

- **Dynamic Modulus Analysis at nm scale**

Berkovich indenter

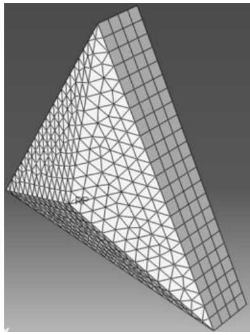

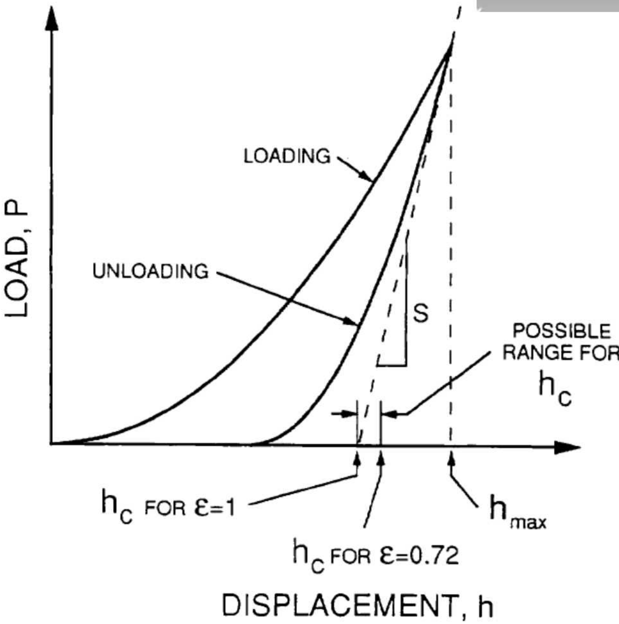

Oliver & Pharr (1992)

Initial Indentation Results

Indentation array: 16 x 16, 20 um spacing
[Hysitron TriboIndenter 900]
Indentation strain rate = 0.1 (Oliver et al., 1997)
(current change in displacement/current total disp.)
Maximum load = 10 mN

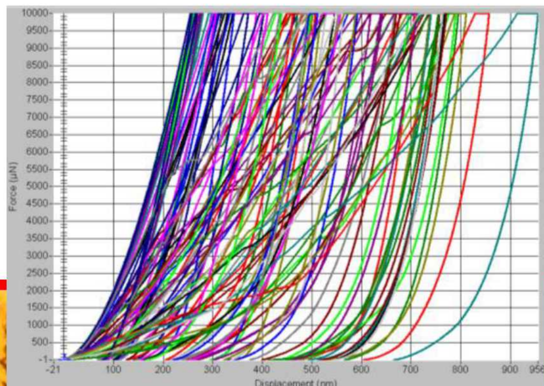

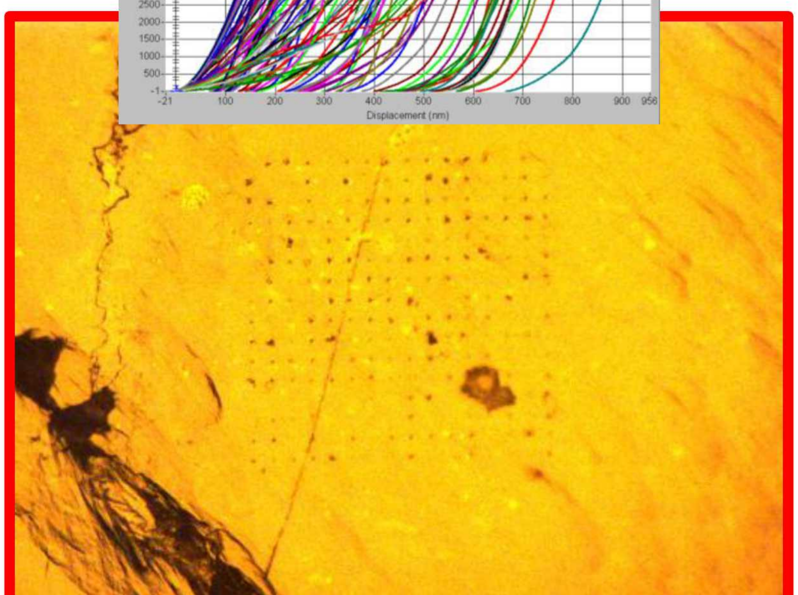

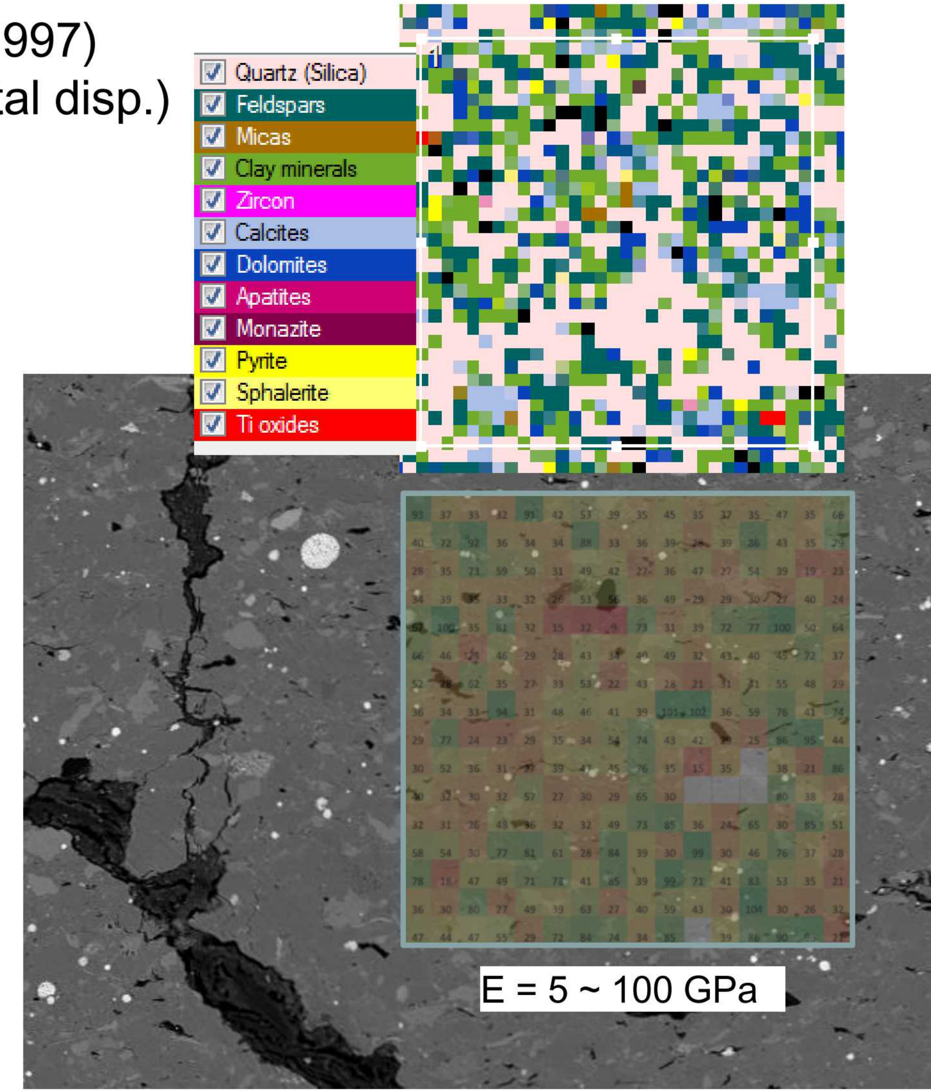

Multiscale Indentation Testing

Loading-unloading cycle

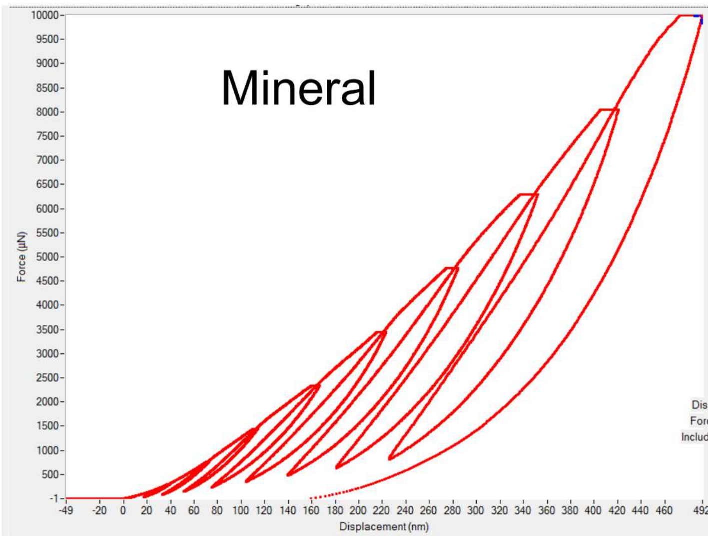

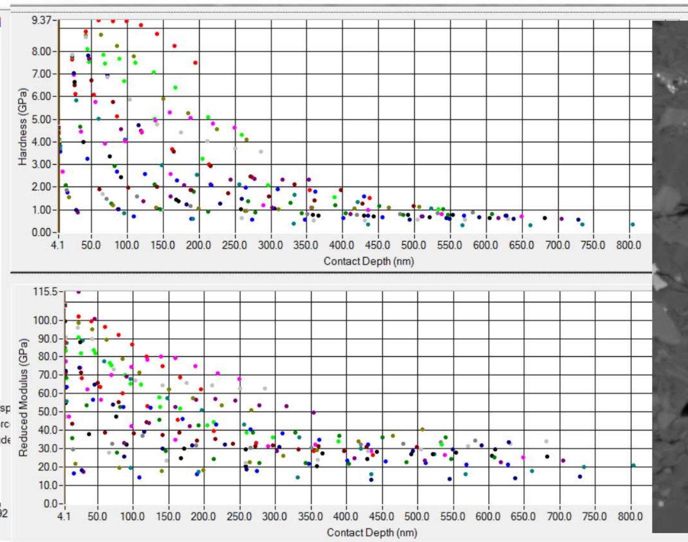

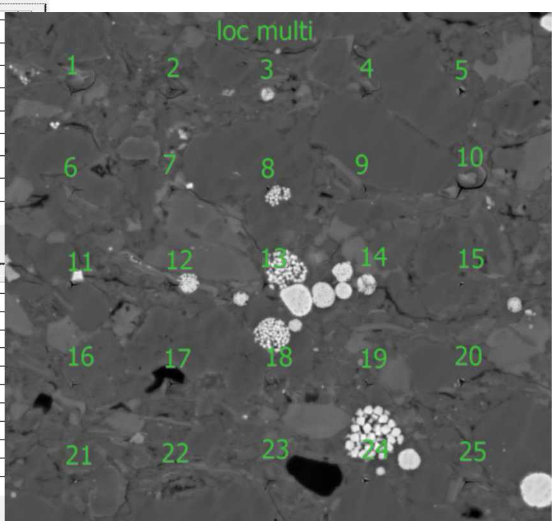

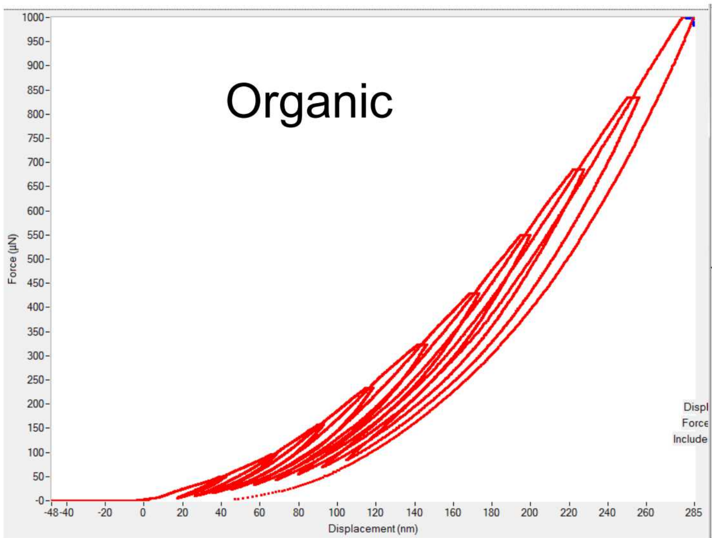

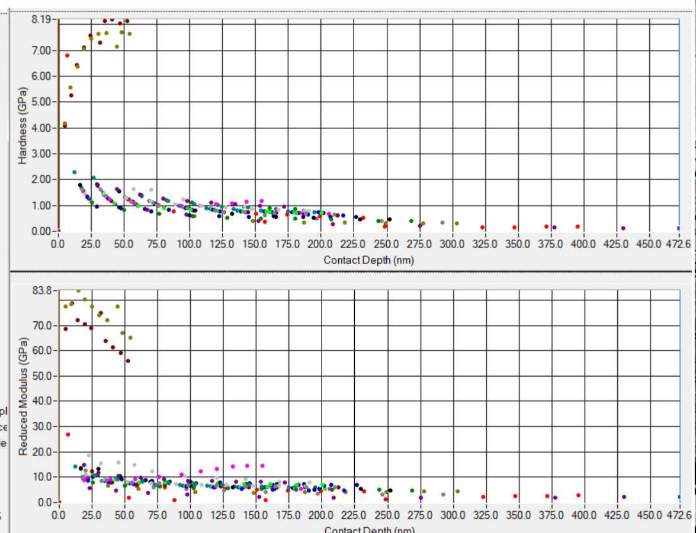

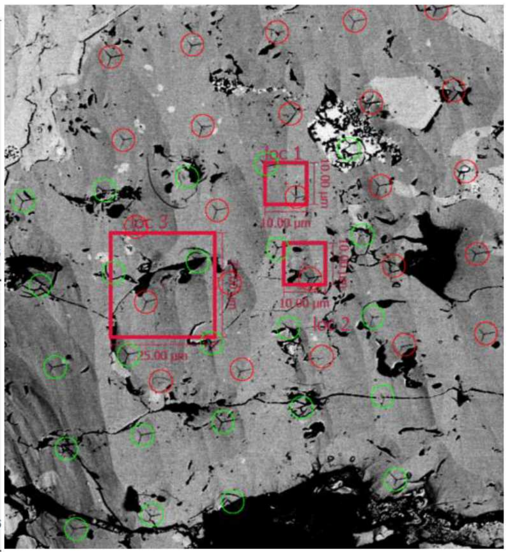

Multiscale Indentation Testing

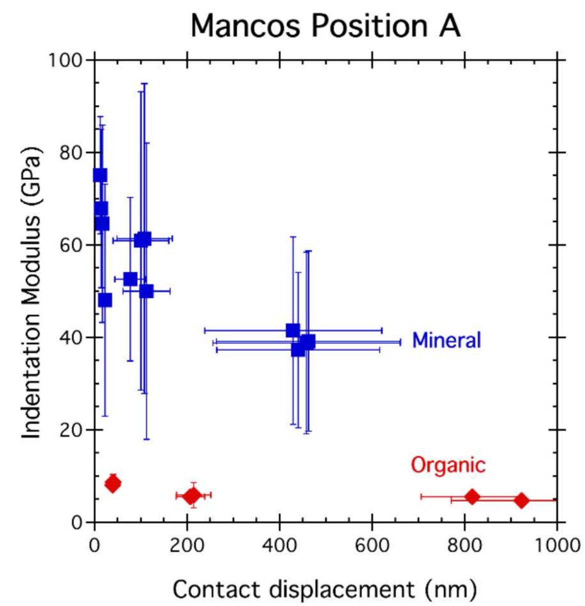

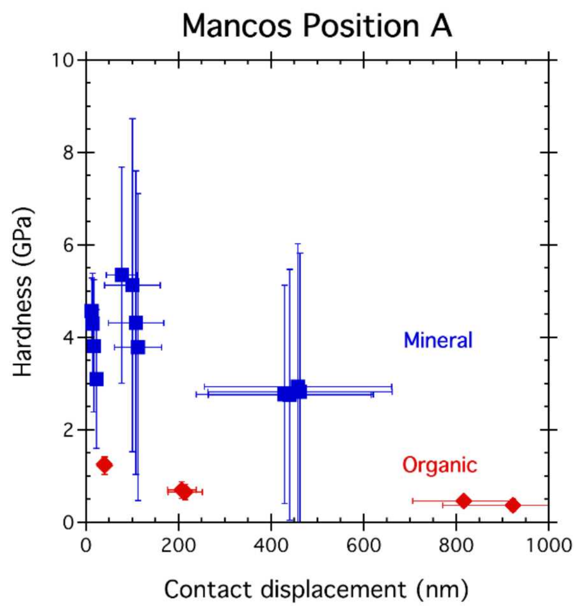

Distributed arrays

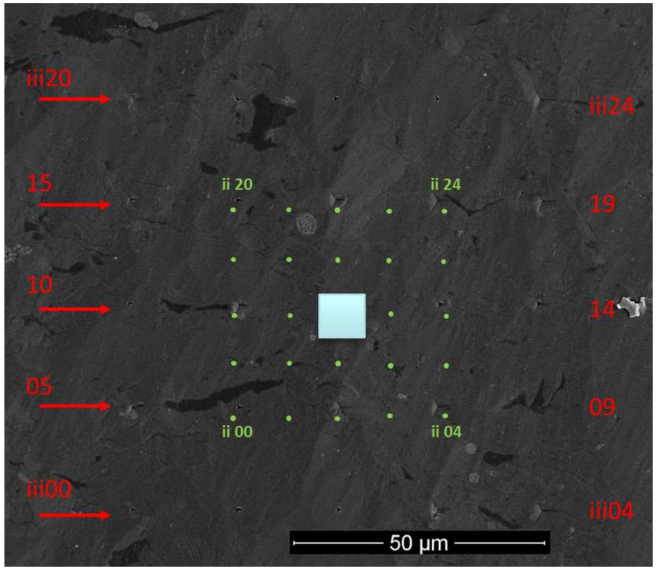

Indentation key	Array dimension	indent spacing	Max Load
i	8x8 um	2 um	0.1 mN
ii	40x40 um	10 um	1 mN
iii	80x80 um	20 um	10 mN

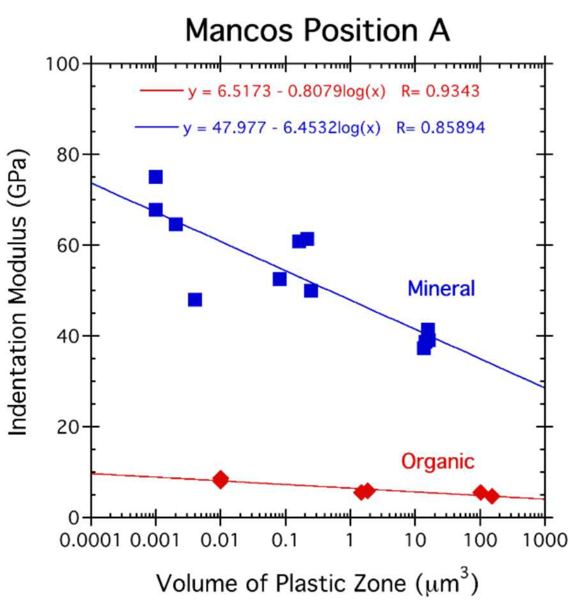

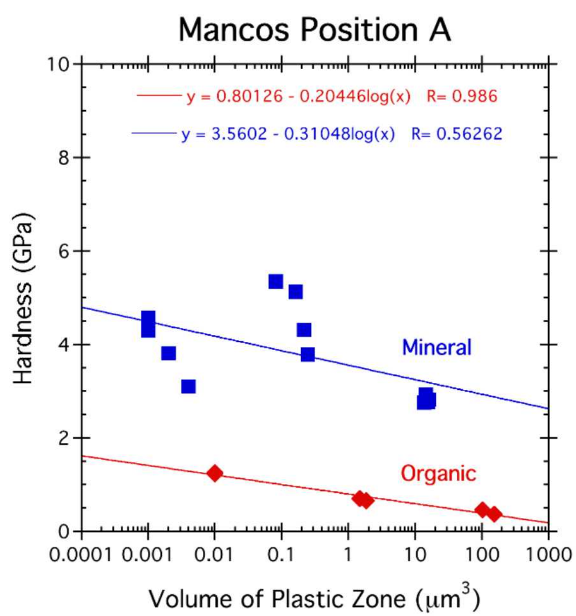

Estimate plastic zone radius

$$\frac{R_p}{\delta_m} = -12.907\frac{H}{E_r} + 4.5451 \qquad \frac{H}{E_r} < 0.35$$

Chen & Bull, Surface & Coatings Technology (2006) 4289–4293.

Effect of Mineralogy on Mechanical Properties

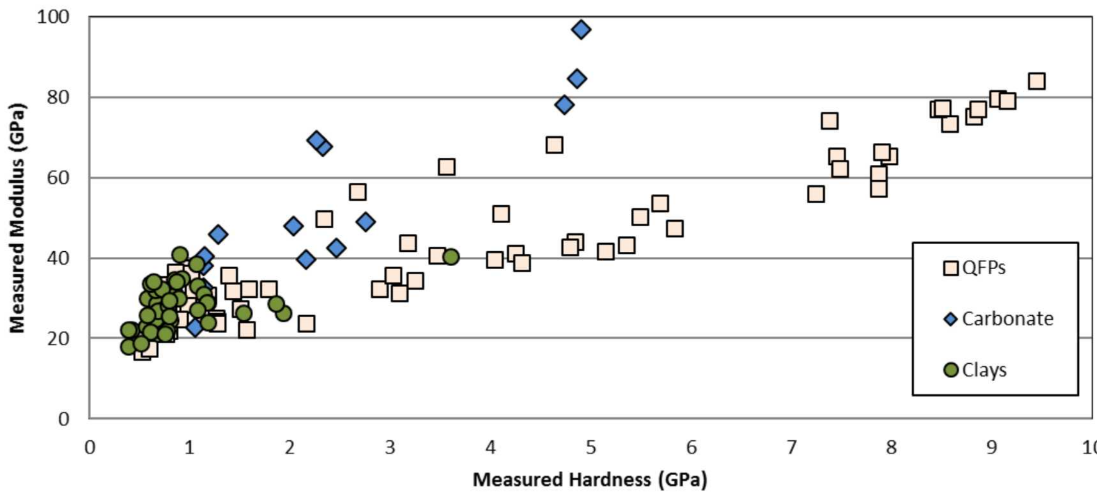

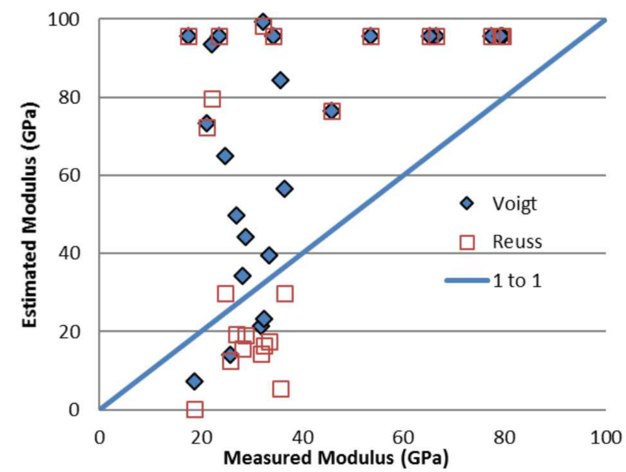

Sone & Zoback (2013)

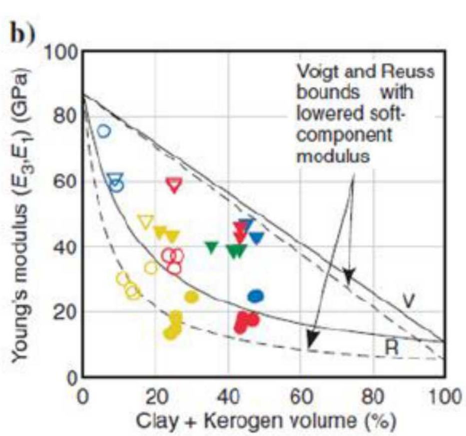

Shulka et al. (2013)

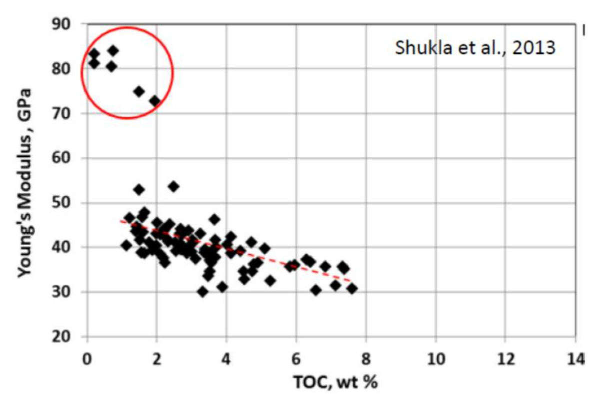

Kumar et al. (2012)

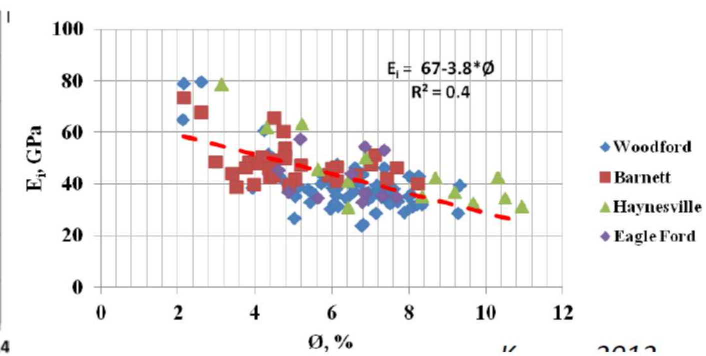

Nanoindentation Impressions

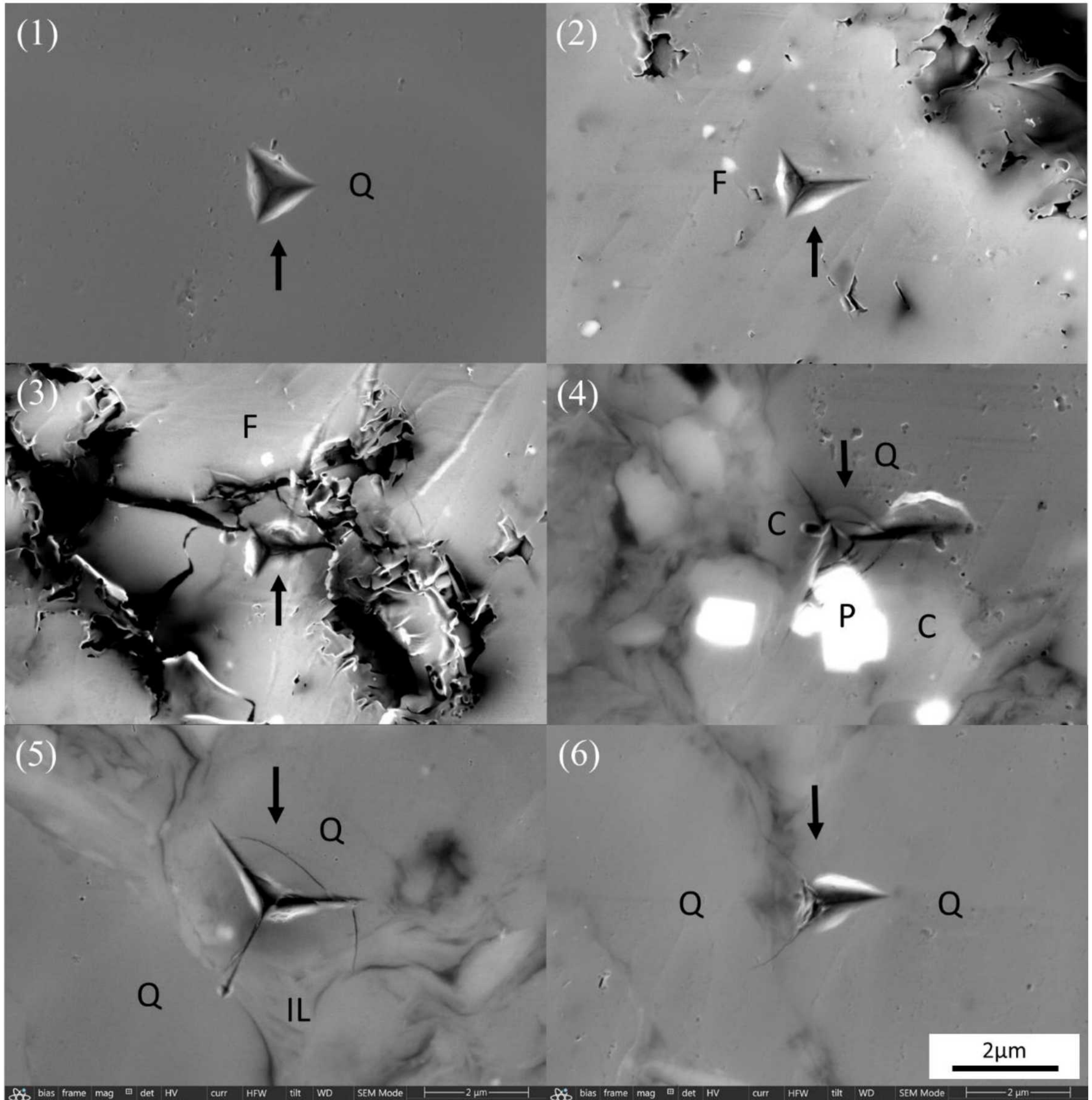

Low-clay percentage samples.
(1&2): surface of pure quartz and feldspar having higher values of mechanical properties such as elastic modulus and hardness.
(3): dissolution surface of feldspar
(4-6): grain-to-grain boundary and edge-of-grain, which have lower mechanical properties values.

NOTE: Q=quartz, P=pyrite, C=carbonate, F=feldspar, and IL=illite)

Yoon et al. (in prep)

Effect of Compositions and textures on Mechanical Properties

High variability

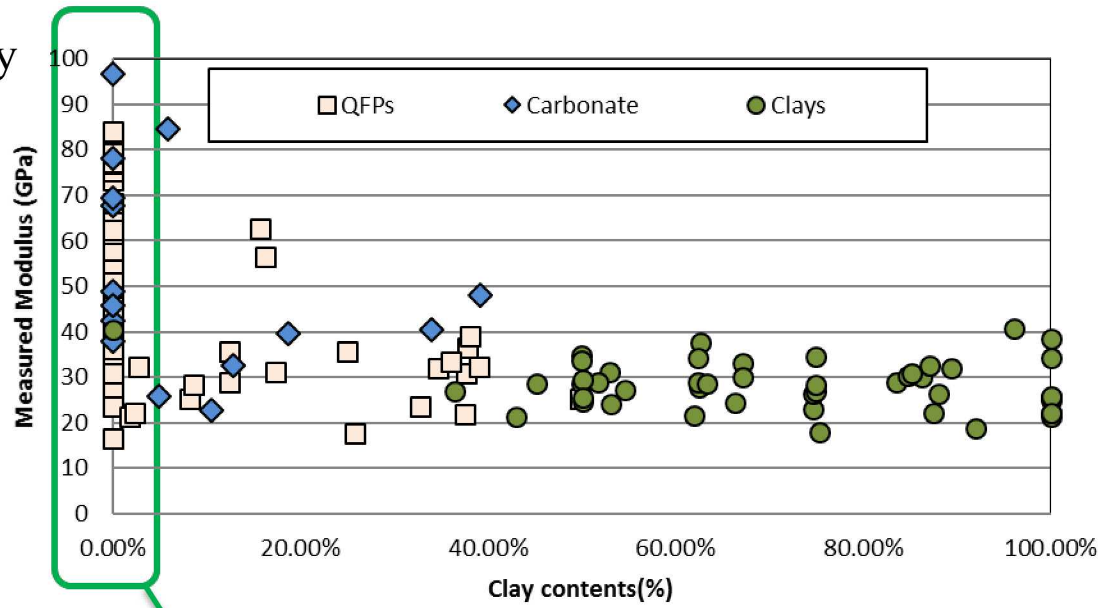

Analysis of SEM image on indentation impressions

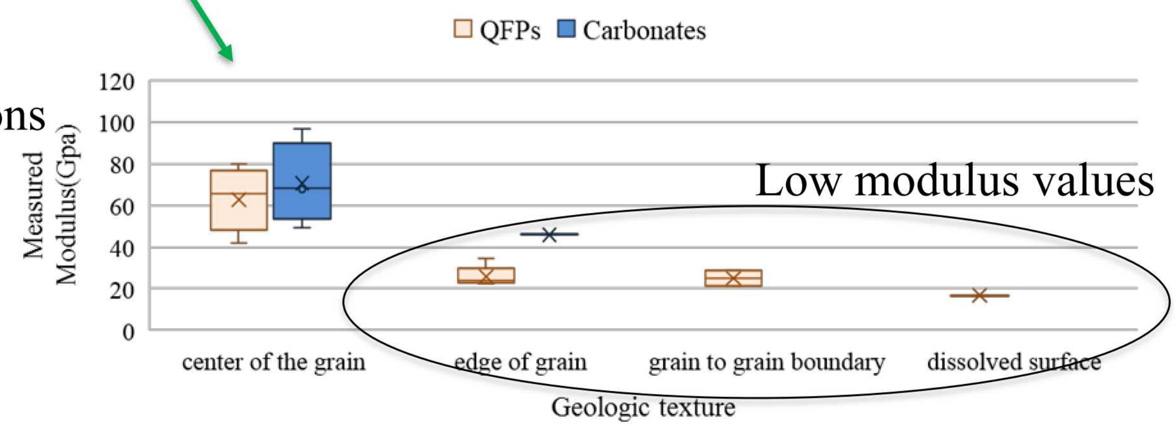

3D Mechanistic Modeling

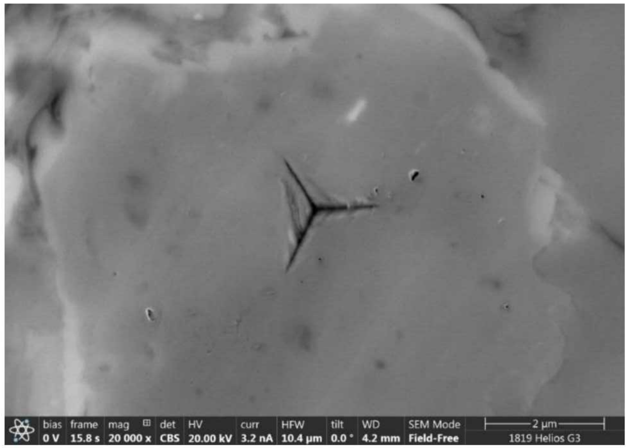

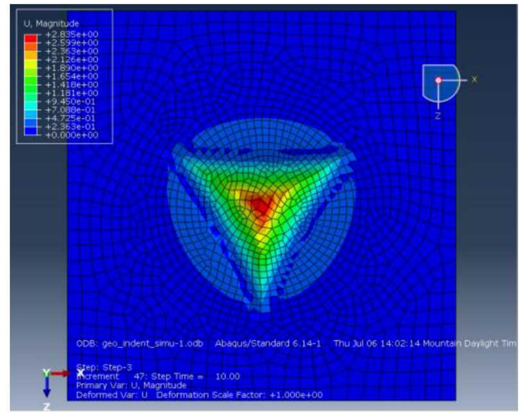

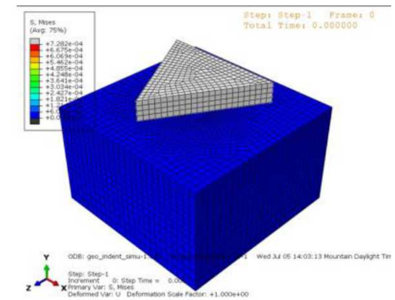

ABAQUS FEA

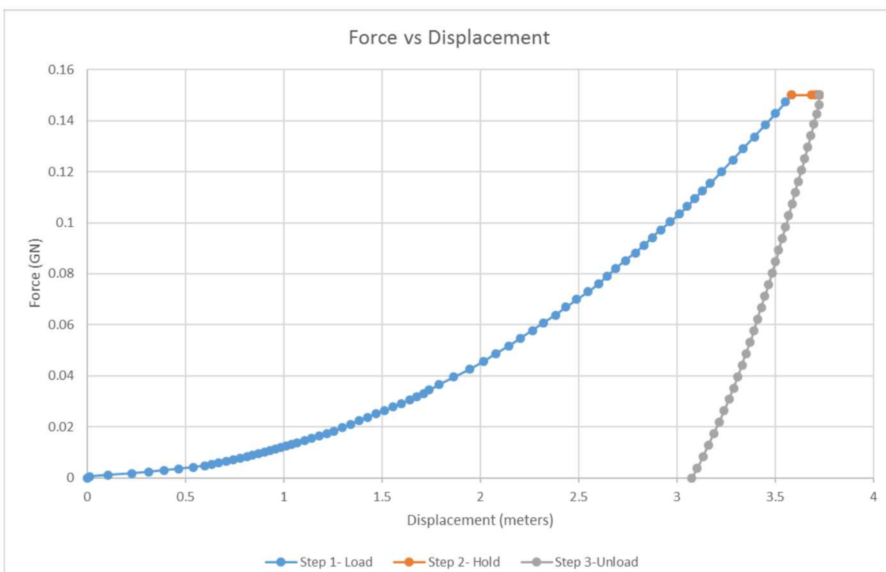

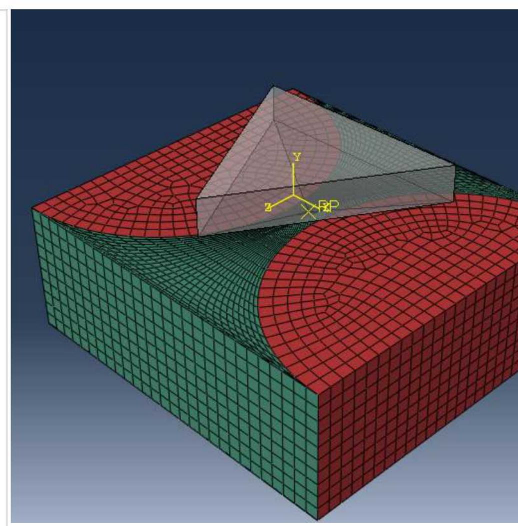

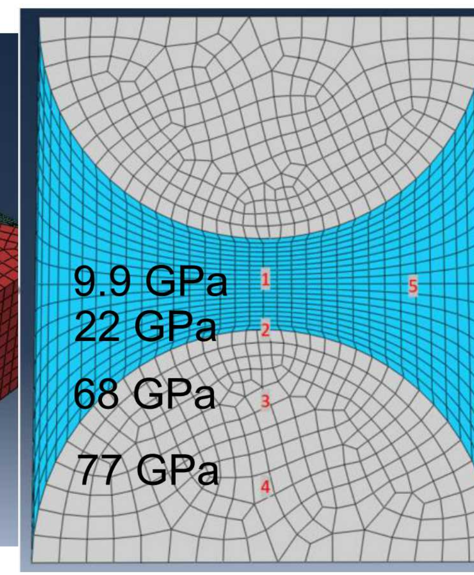

Elastic Modulus

Upscaling for Mechanical Properties

- Phase field modeling for averaging mechanical properties
  - Spatial mineralogical mapping with compositional heterogeneity
  - Development of correlation with nanoindentation results
  - Evaluation of soft cement or multi-mineral regions on mechanical responses with various conditions (e.g., defects, layering, anisotropy)

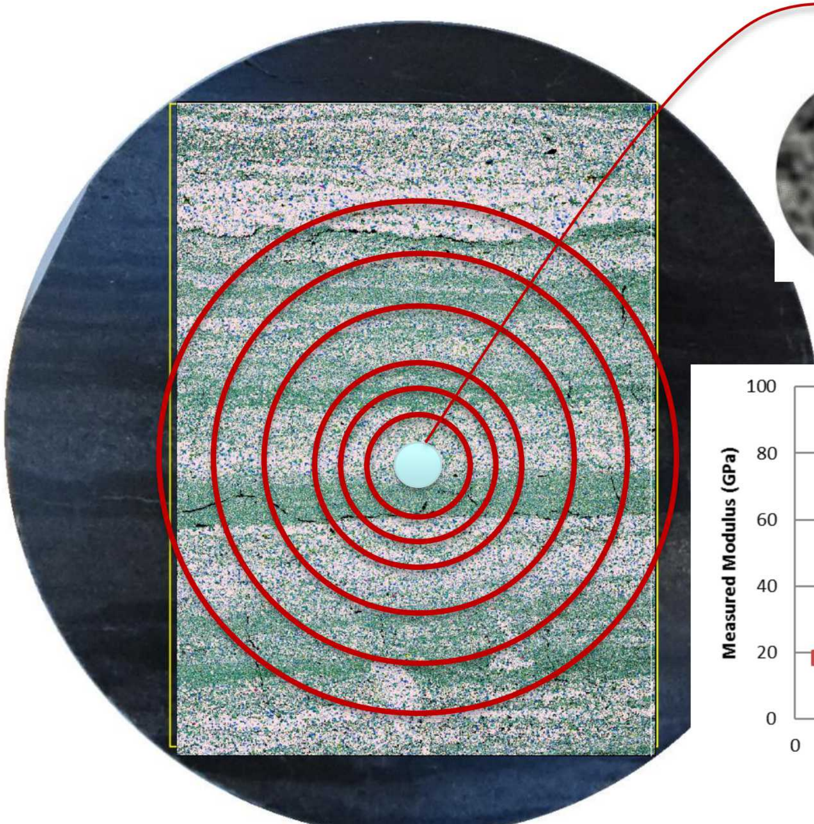

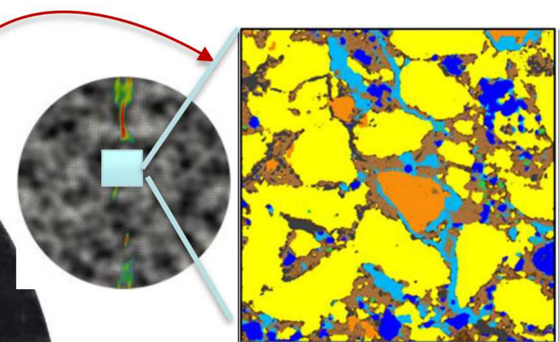

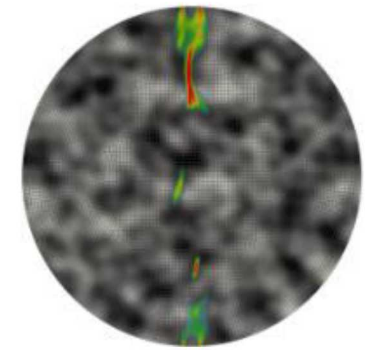

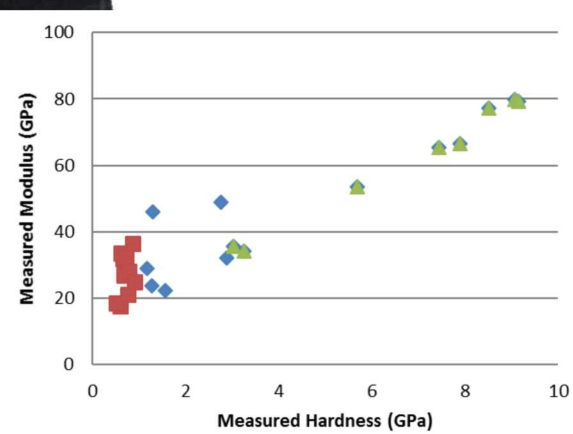

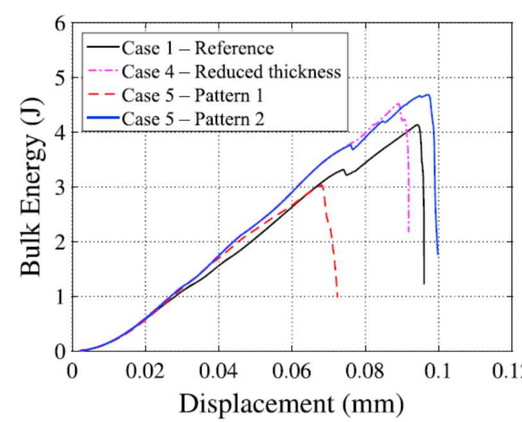

Velocities of Mancos Shale lithofacies

Drilled Core Samples

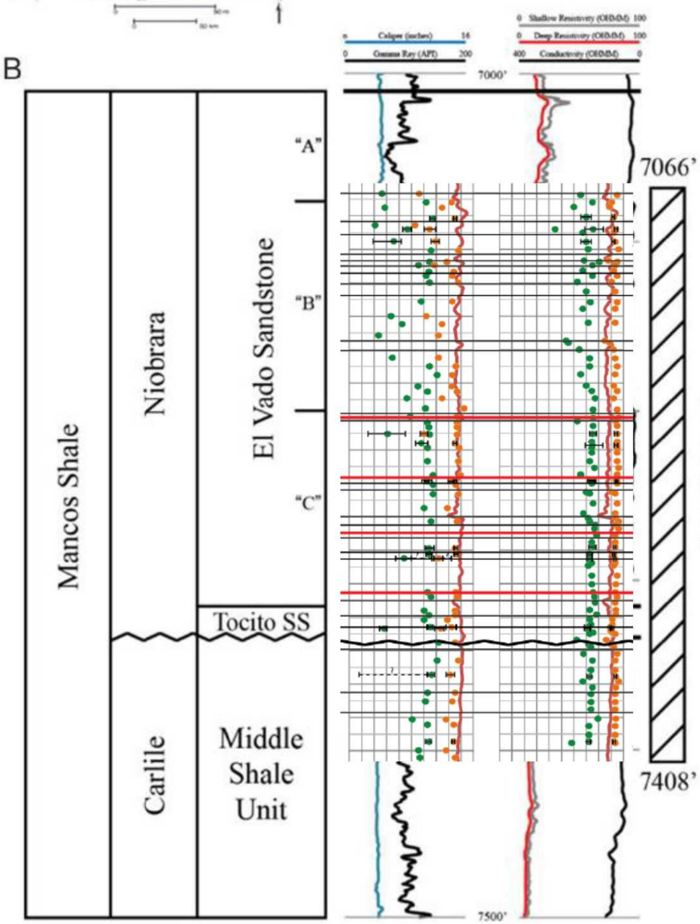

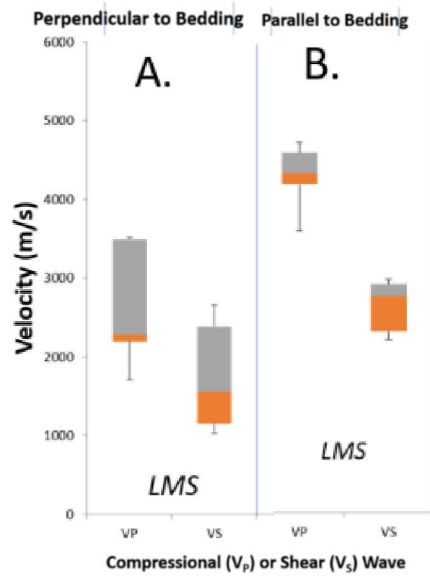

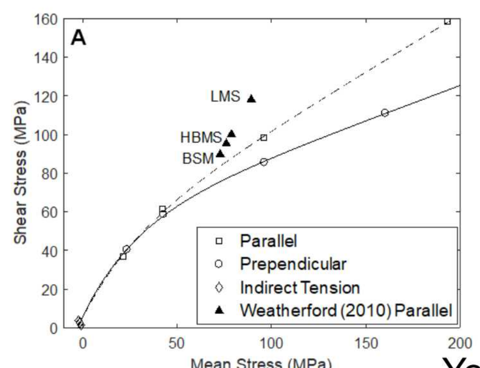

Lab Block Samples

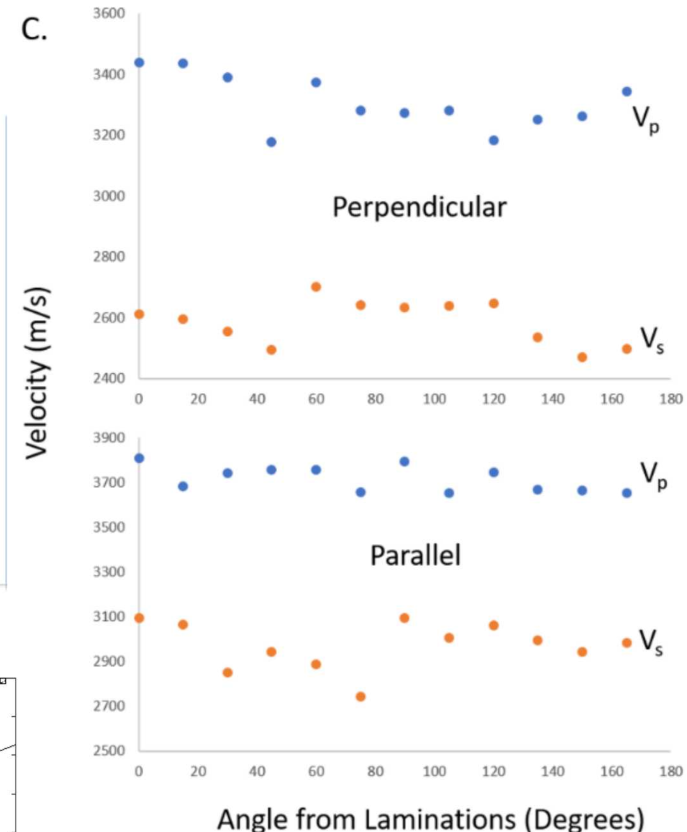

Yoon et al. (AAPG, Memoir 2019, in press)

Other Ongoing Works

Chemo-mechanical Processes: Chemical Flooding in Nano-porous Chalk

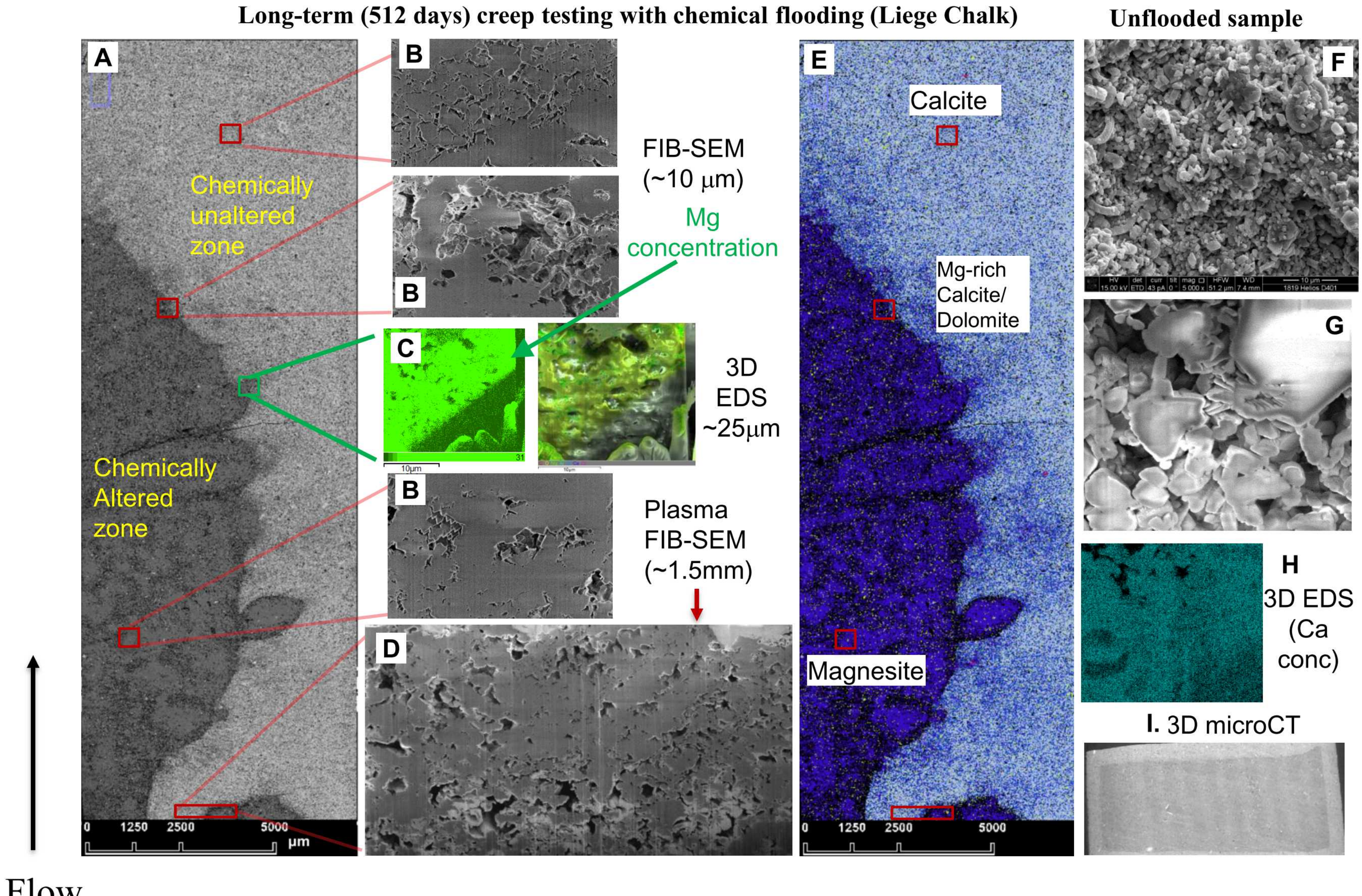

Samples from Nermoen et al., (JGR,2015)

Yoon et al. (In prep)

Experimental Simulations of Borehole Breakout

- Borehole breakouts used to determine reservoir stress states
  - Errors can be high as 30-40% (JASON, 2014)
- Developed novel technique to investigate behavior in laboratory
- Experiments investigated chemistry and anisotropy effects on borehole breakout
- Continue development to simulate hydraulic fracturing

Prepped Mancos Shale sample

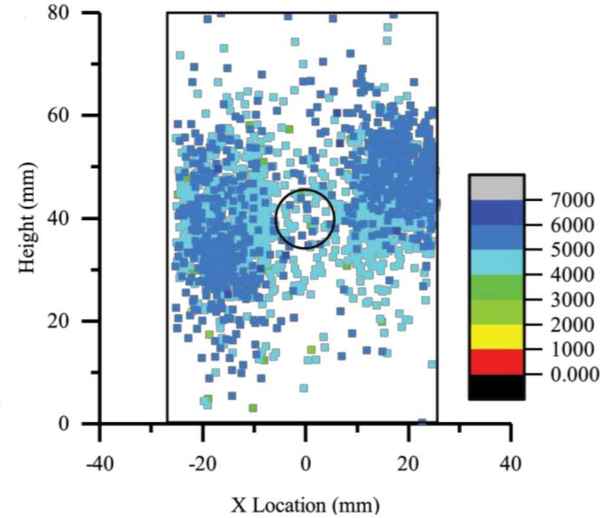

Acoustic emission location in Sierra White Granite Experiment

Borehole breakout in Mancos Shale

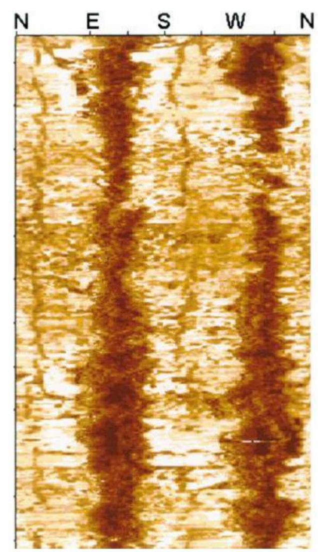

Ultrasonic televiewer image of wellbore, Zoback et al., 2003

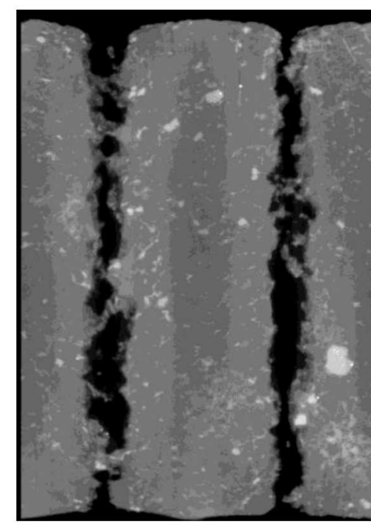

CT image from experiment in granite

Choens et al. (In prep)

In-Situ Fracture Toughness

- Novel testing apparatus capable of measuring fracture toughness at in-situ conditions
- Designed to fit inside of titanium pressure vessel
  - Pressure, temperature, chemistry
- Utilizes short rod geometry
  - Investigated toughness in sandstone, shales
- Measure fracture roughness with 3D surface profilometer
- Demonstrated differences in fracture toughness for wet, dry supercritical CO_2

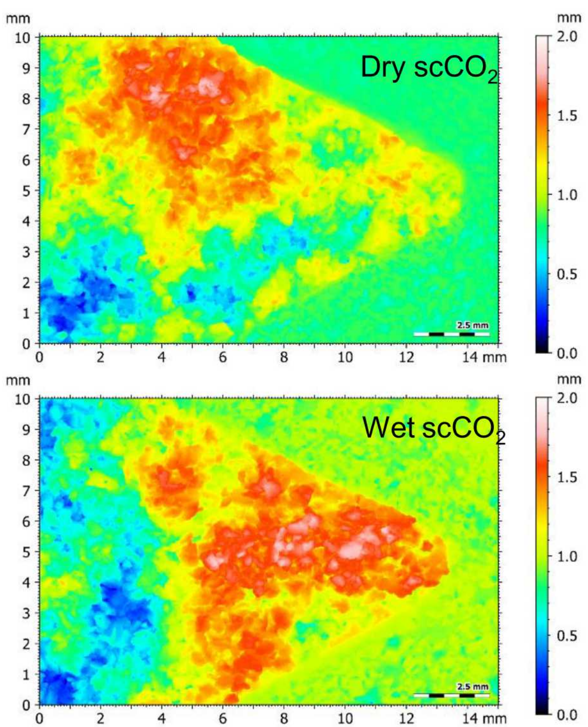

Chevron Notched Testing

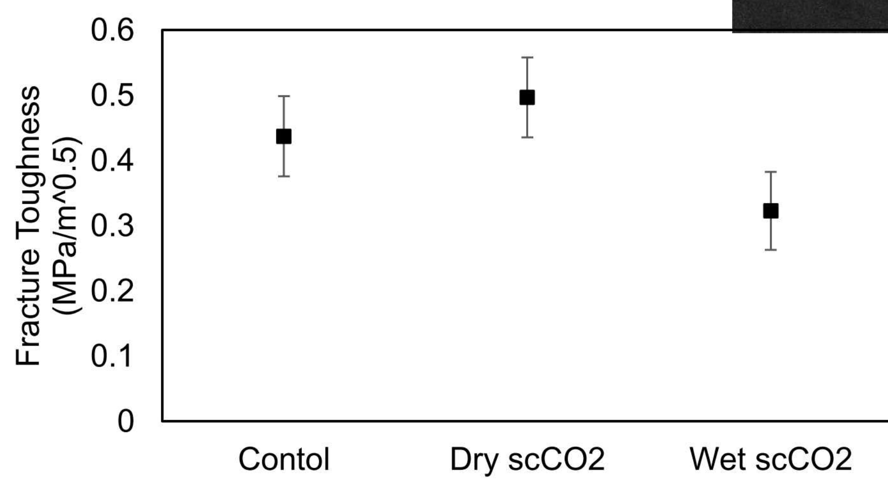

Choens et al., 2017, EFRC PI meeting

Geomechanical characterization of outcrop, core samples

- Pre-feasibility study for CO_2 sequestration for Utah coal power plants
- Measure surface hardness, acoustic velocities of cores, outcrop
- Combine with sed facies
- Integrating core, outcrop, laboratory data

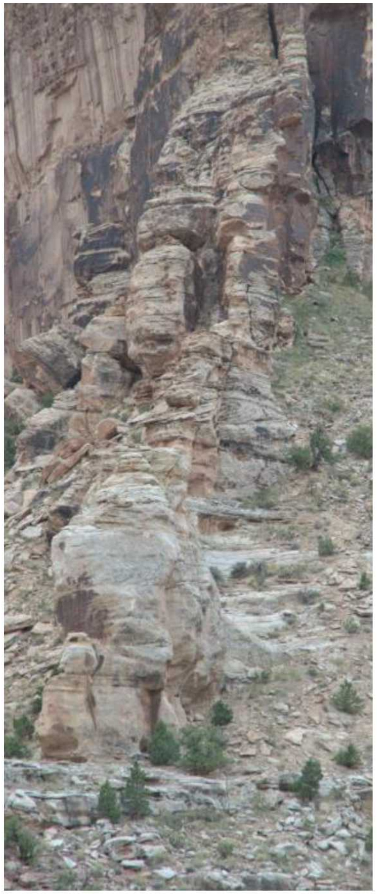

Outcrop of the Upper Navajo, Buckhorn Wash, Utah

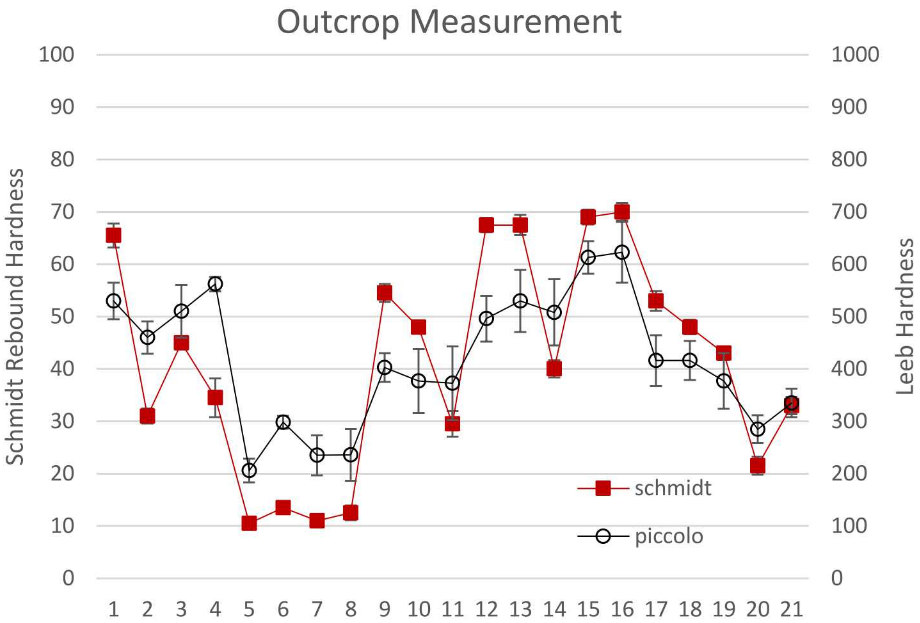

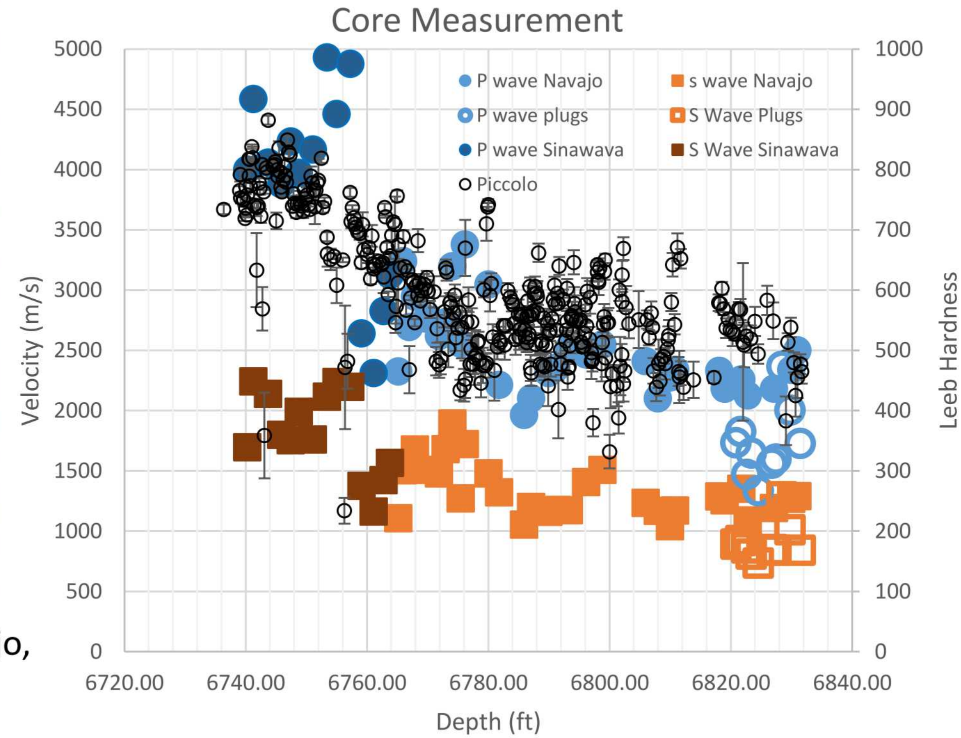

Choens et al. work

Fracture Patterns: Borehole Breakout Test

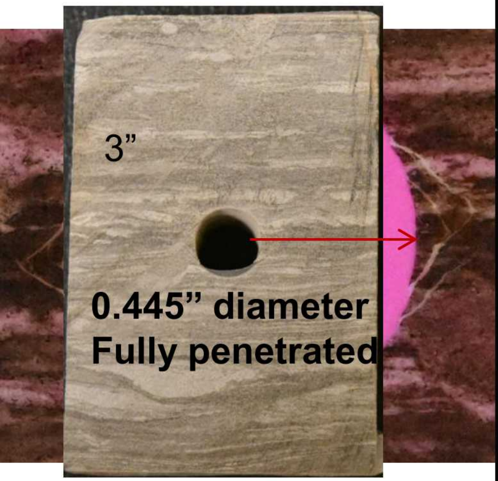

2” diameter

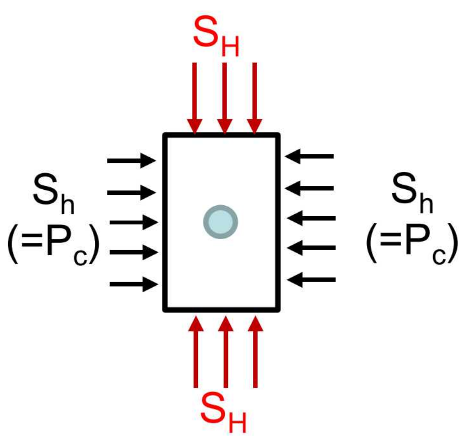

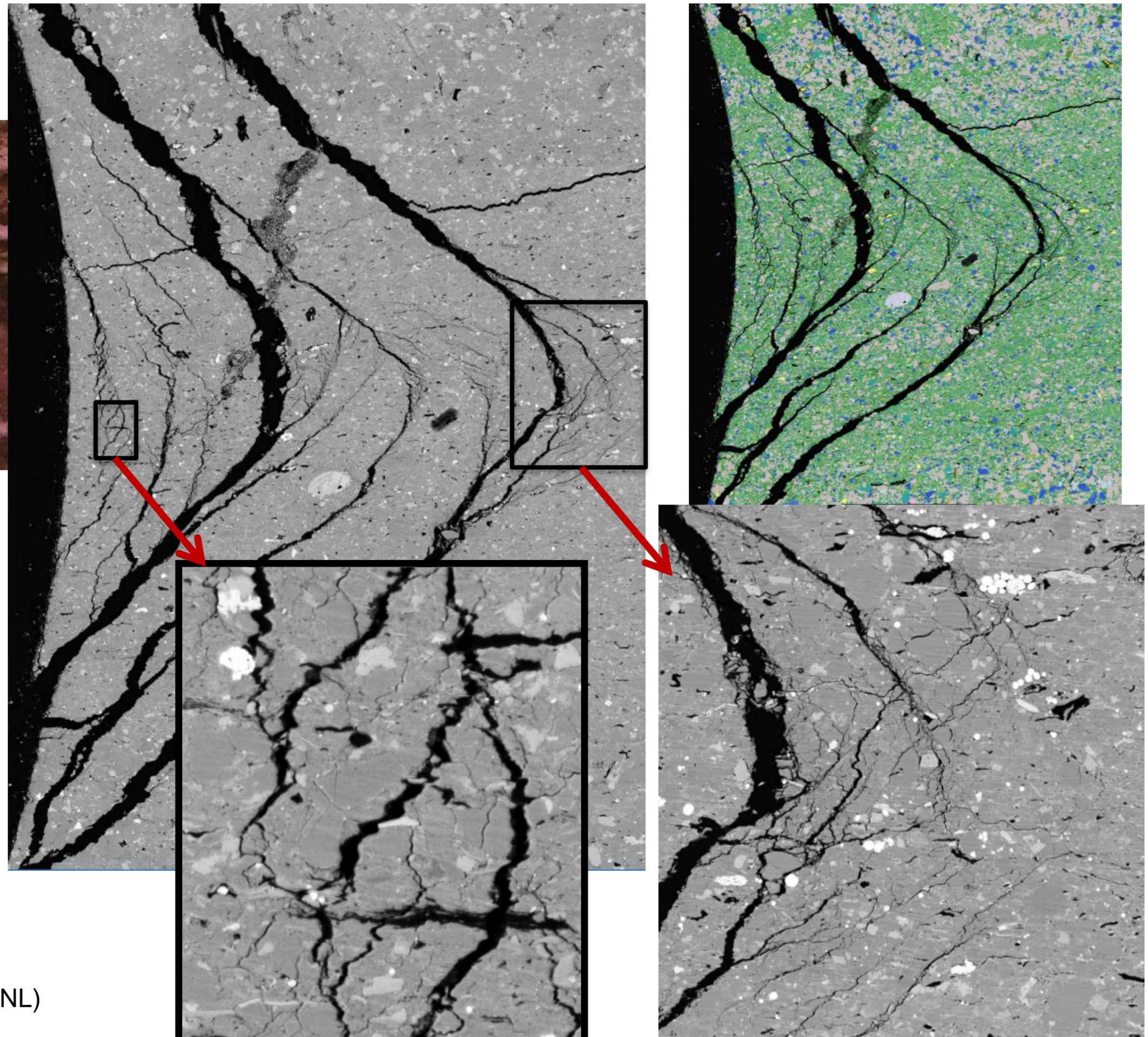

Experiment by R.C. Choens (SNL)

Permeability Control and Proppants' Behavior in Fractures

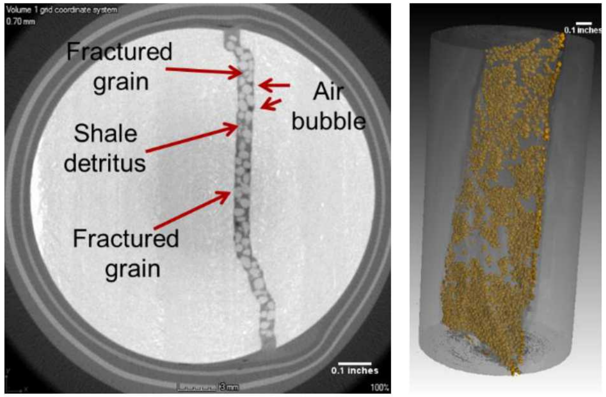

Micro-CT image with proppants in a fracture

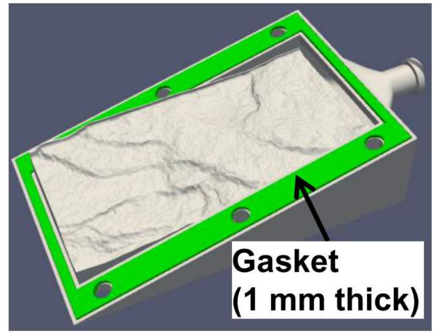

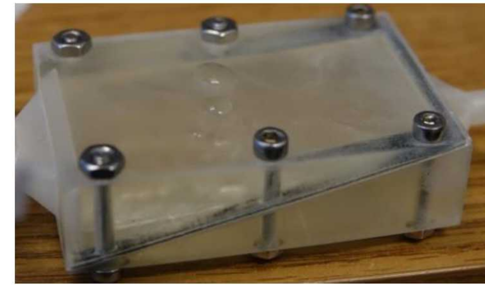

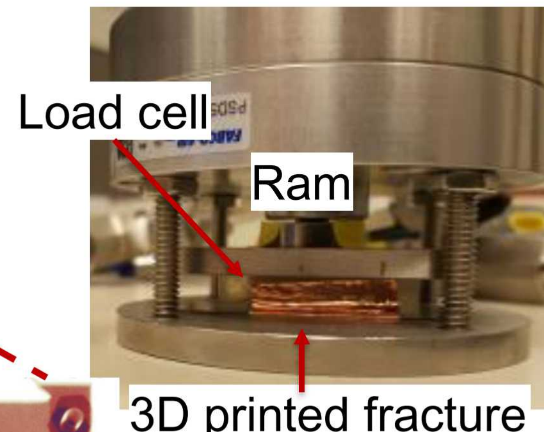

3D printing applications

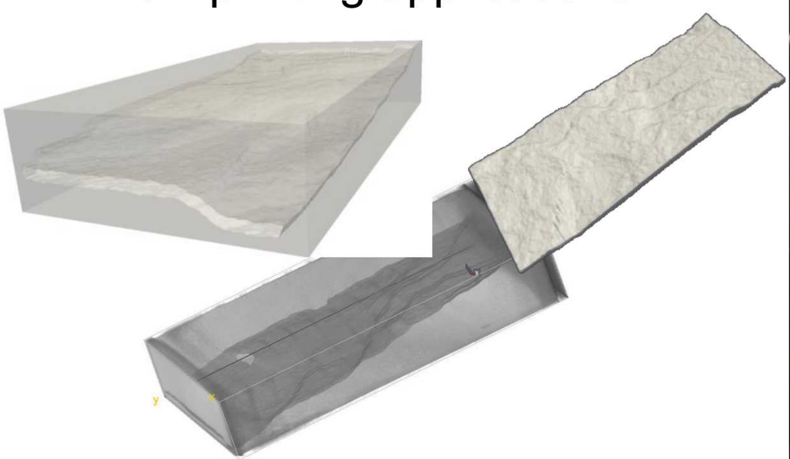

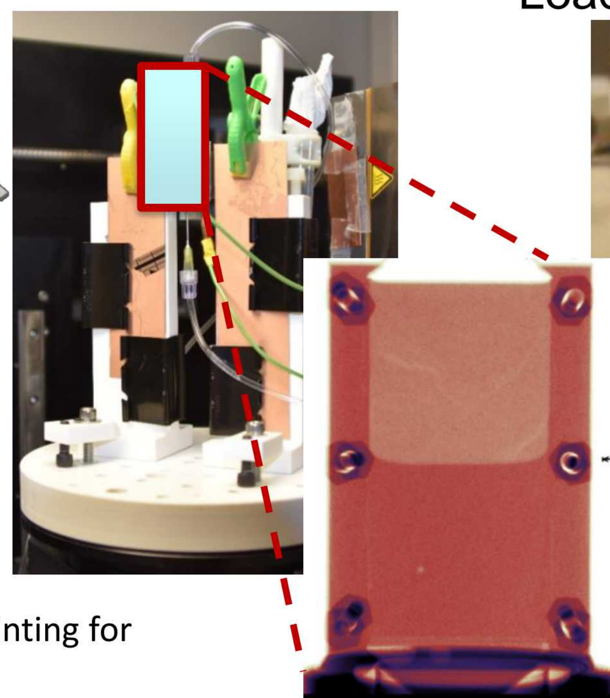

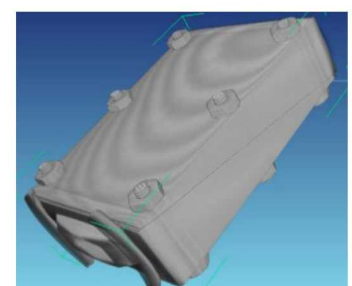

SAND 2017 report: Digital Rock Physics and 3D Printing for Fractured Porous Media (Martinez et al., 2017)

Multiphysics Simulations

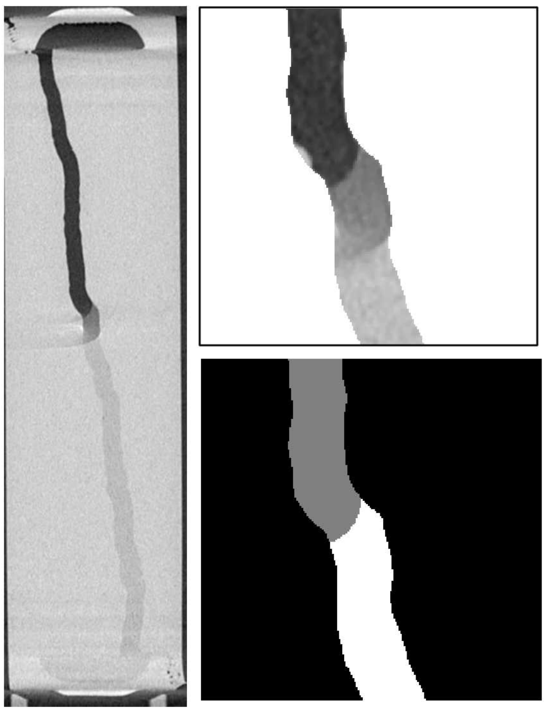

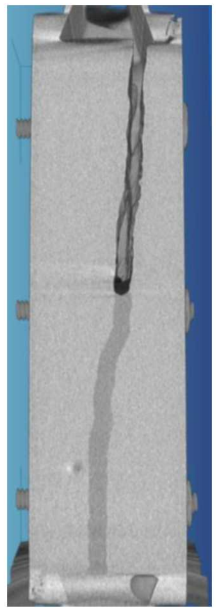

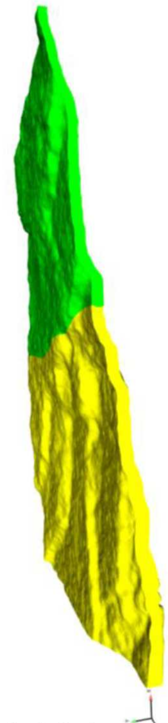

Multiphase flow

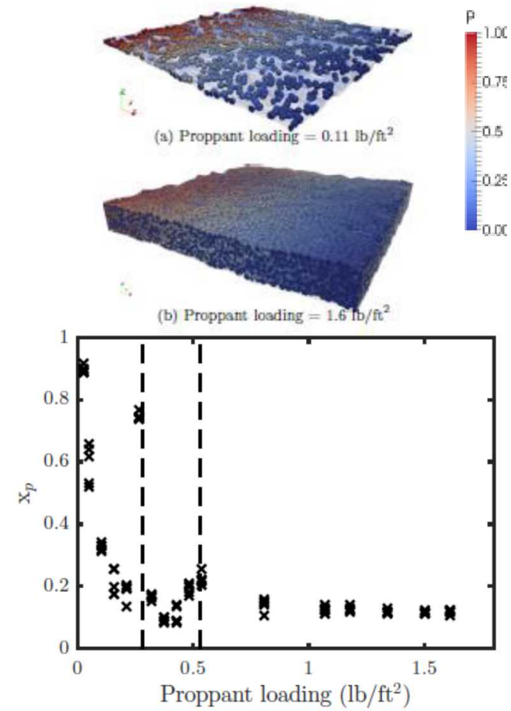

Proppants' behavior (Bolintineanu et al., 2017, IJRMMS)

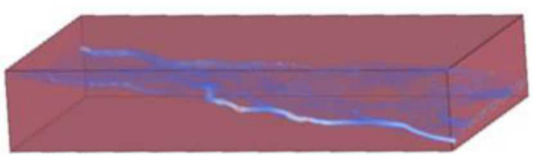

CFD simulation flow field

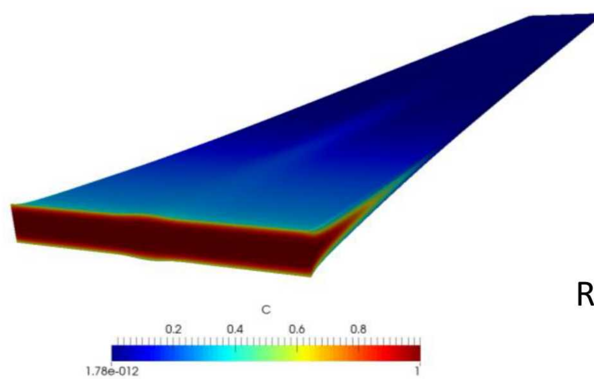

Reactive Transport

Methane flow in kerogen "tubule"

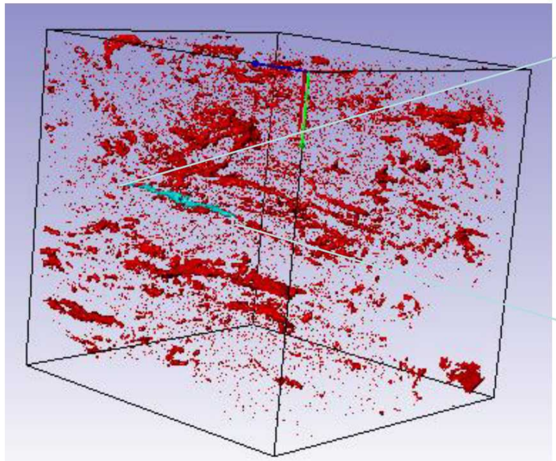

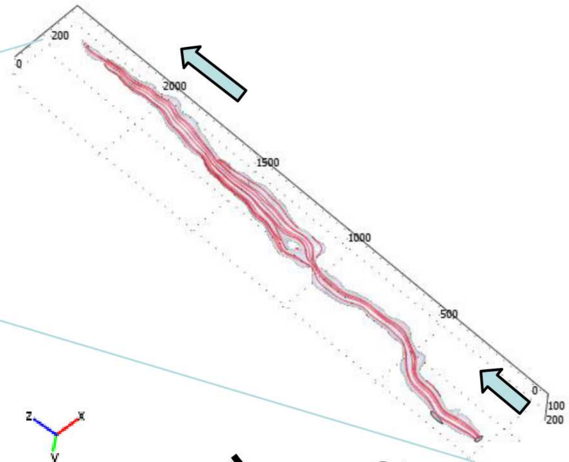

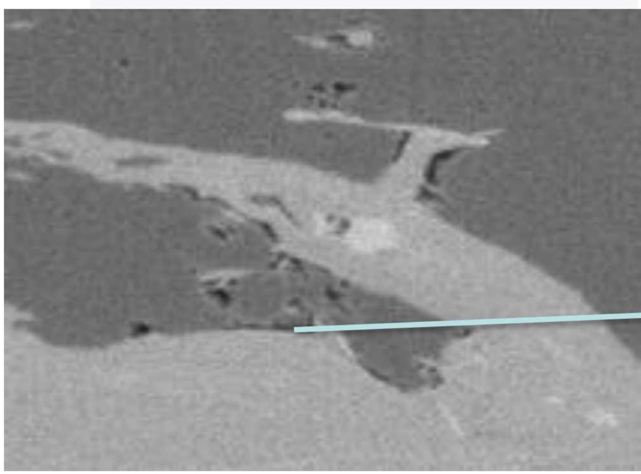

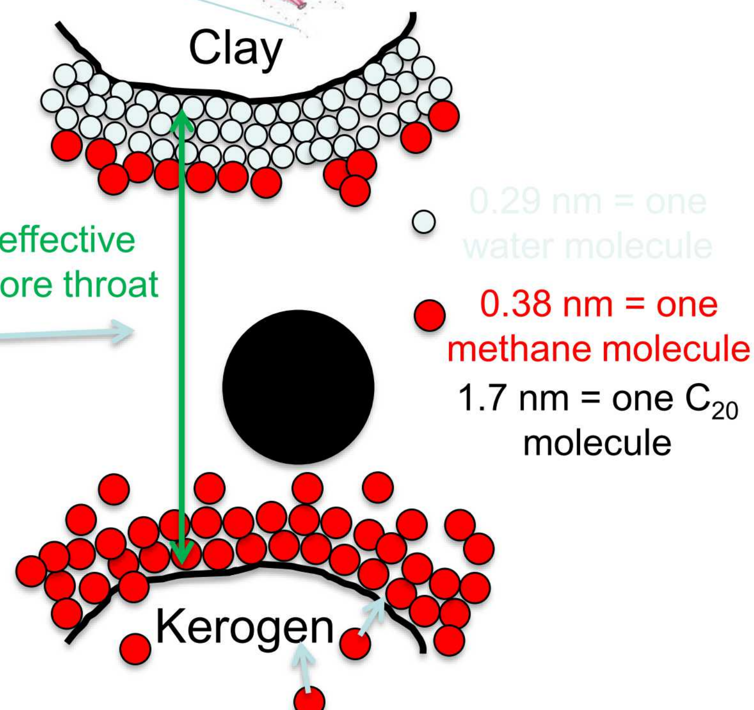

Pore throats are at molecular scale

Dewers et al. (2018, AGU monograph)

Seismic Signal Acquisition and Analysis

- Full waveform measurements with AE and seismic wave transmission/reflection:
  - Delineate the stages of crack initiation and propagation
  - Use bi-& tri-axial loading conditions and crack orientations to achieve mixed-mode I-II-III loading with and without pore pressure

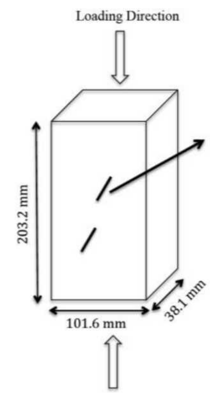

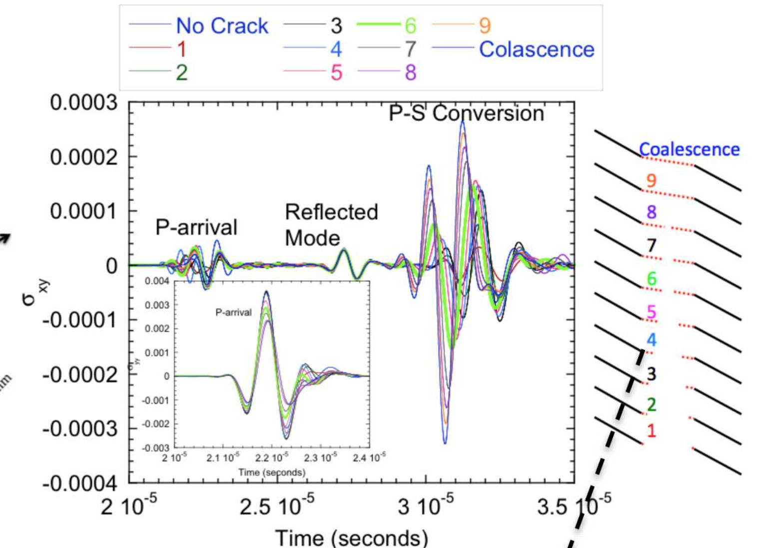

- Experimental data will be analyzed in conjunction with computer simulations:
  - Identify all possible components of the signals (body wave, converted modes, guided modes, etc.)
  - Interpret the hydraulic properties of fractures
  - Develop the relationship between the interpreted stiffness of the fractures and fluid flow (w/ micro-CT images)

Simulated shear stress wavefront propagating from bottom to top (Pyrak-Nolte at Purude)

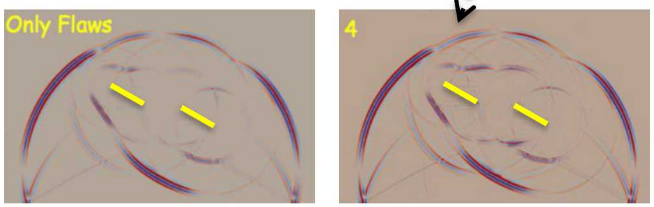

Fully coupled poroelastic simulation of fluid-injection scenarios (Chang et al., BSSA 2018, JGR & GRL (under review)

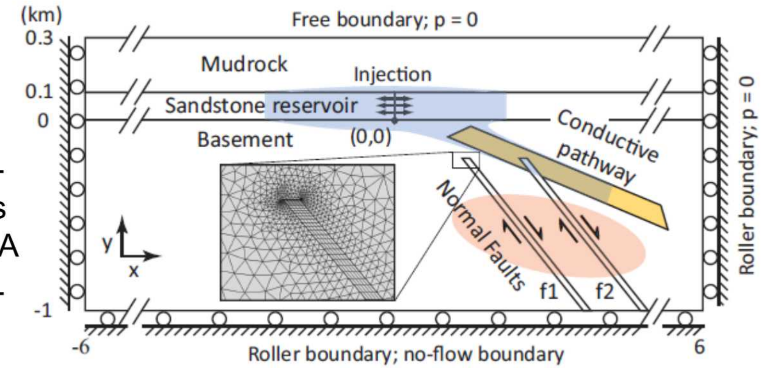

Poroelastic coupling effect on injection-induced seismicity

▶ Strike-slip fault(s) are modeled in a 2-D aerial-view domain including poroelastic coupling with the single-phase flow

▶ Injection for 5 days with the rate of 0.1 [kg/m/s], simulation runs for 10 days to evaluate post shut-in behaviors

▶ Coulomb stress change ($\Delta\tau = f\Delta p + (\Delta\tau_s + f\Delta\sigma_n)$) from the initial stress state is obtained (normal stress: positive for tension)

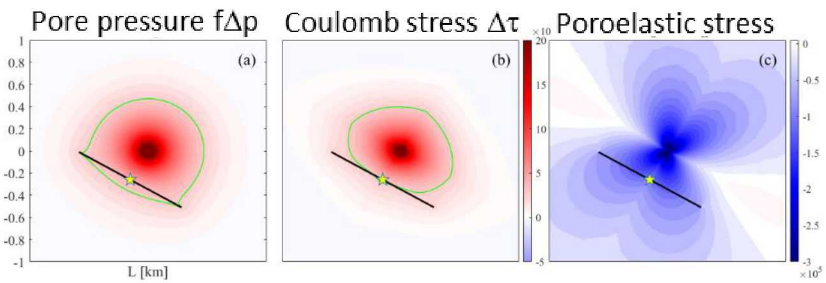

★ = location where pressure and stresses are obtained

— contour value of 0.3 MPa

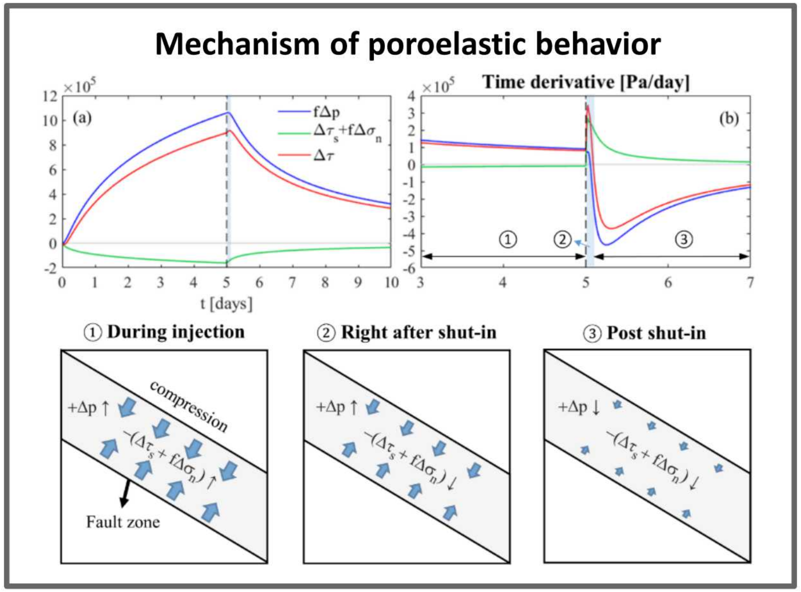

▶ The seismicity rate R is estimated based on $\Delta\tau$ (Segall & Lu, 2015)

$$\frac{dR}{dt} = \frac{R}{t_a}\left(\frac{\dot{\tau}}{\dot{\tau}_0} - R\right)$$

t_a: characteristic relaxation time

$\dot{\tau}$: stressing rate (0=background)

▶ Sensitivity tests on locations and the number of the fault with respect to the injection well show that

1. Closer to the injector, faster pressure buildup causes higher R

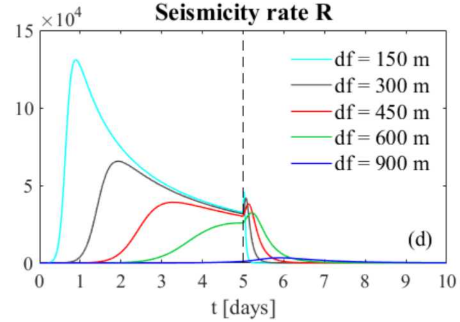

df = distance between fault and injector

2. The additional high-permeability fault acts as a mechanical or hydraulic cushion for pressure buildup while the low-permeability (sealing) fault confines pore pressure propagation

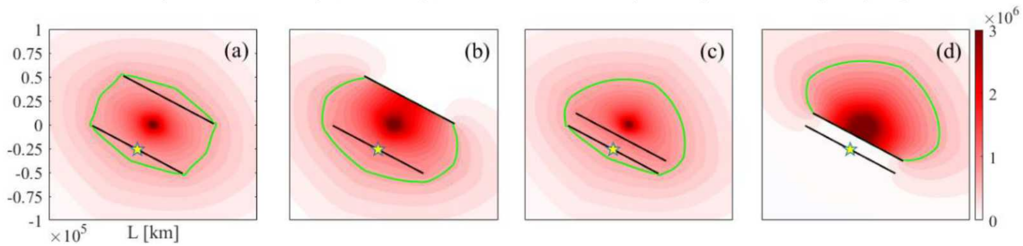

(Chang et al., BSSA 2018
Chang and Yoon, JGR & GRL, under review)

Machine Learning INTRODUCTION

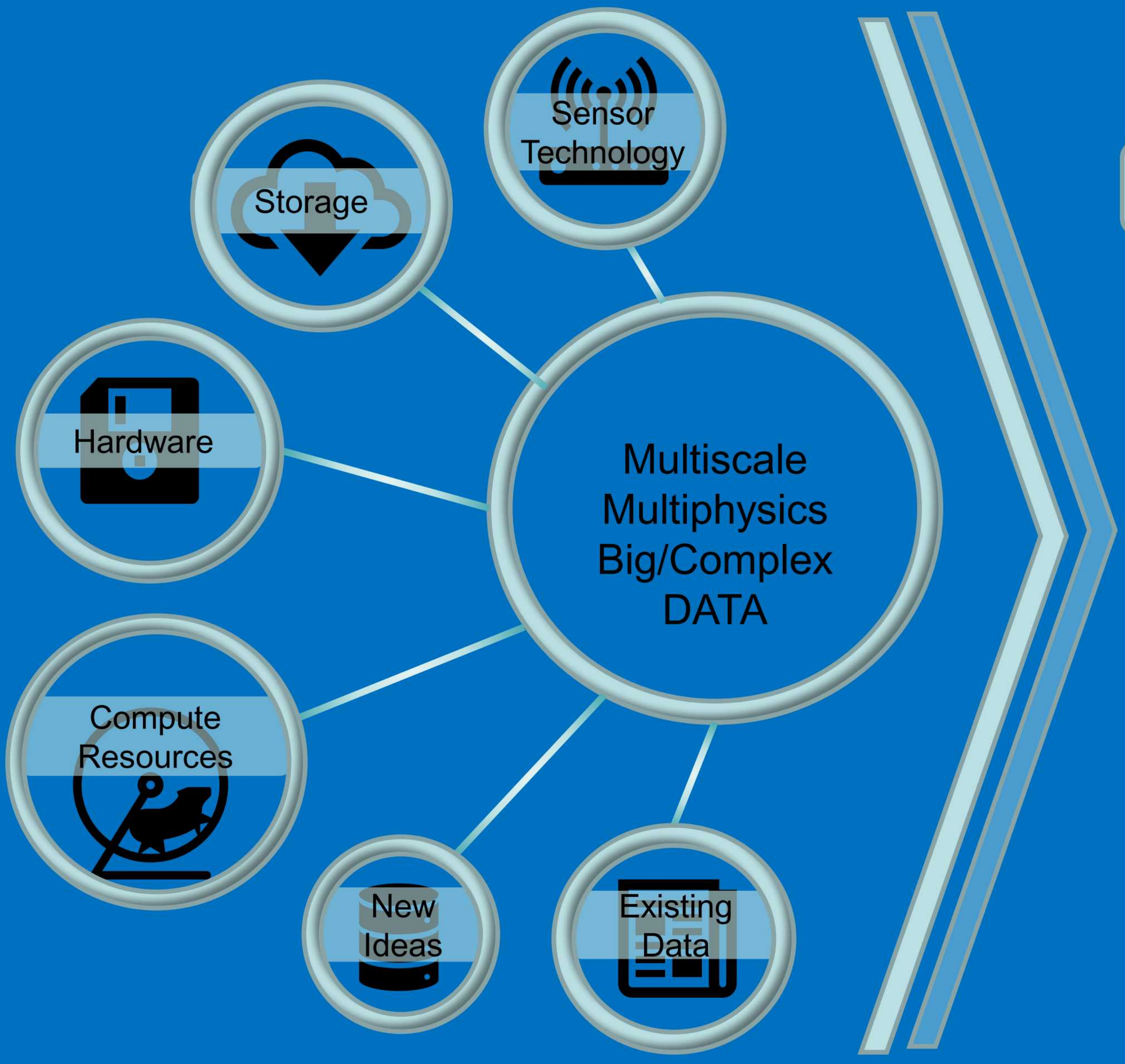

ANALYSIS

Visualization

Better Models

More Accurate Predictions

Patterns/Attributes

Reduce Latency

FE CHALLENGES

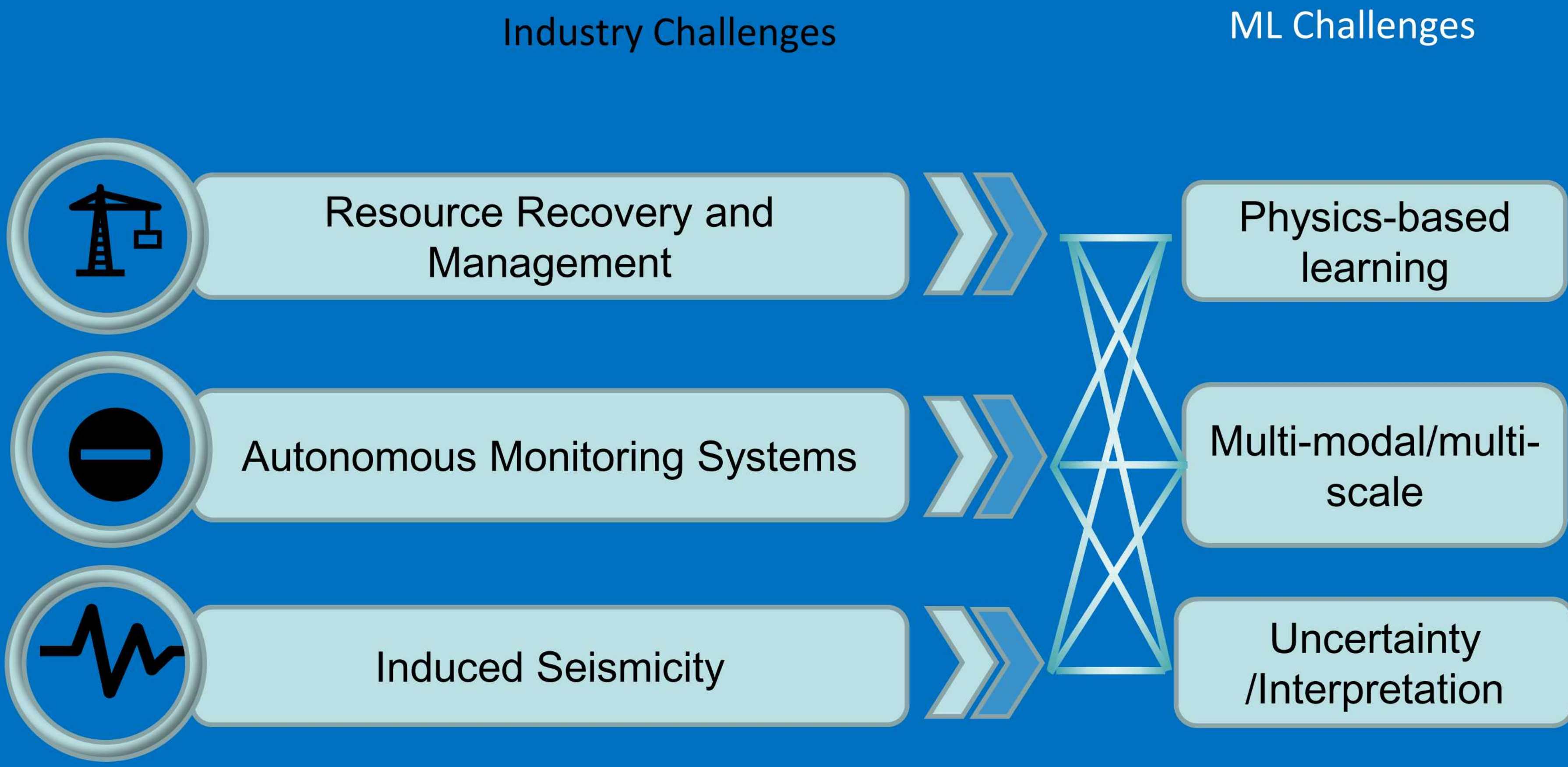

SANDIA'S MACHINE LEARNING ENVIRONMENT

ECP
EXASCALE COMPUTING PROJECT

HPC

MLaaS

MACHINE LEARNING & DEEP LEARNING
MLDL

Combining Sandia's Strength in Geoscience with Resources and Partnerships that Enhance ML outcomes

PREDICTIVE DATA-DRIVEN PLATFORM FOR SUBSURFACE ENERGY PRODUCTION

Goal: Match production history + increase portability

Targets: multiscale, physics + data driven learning

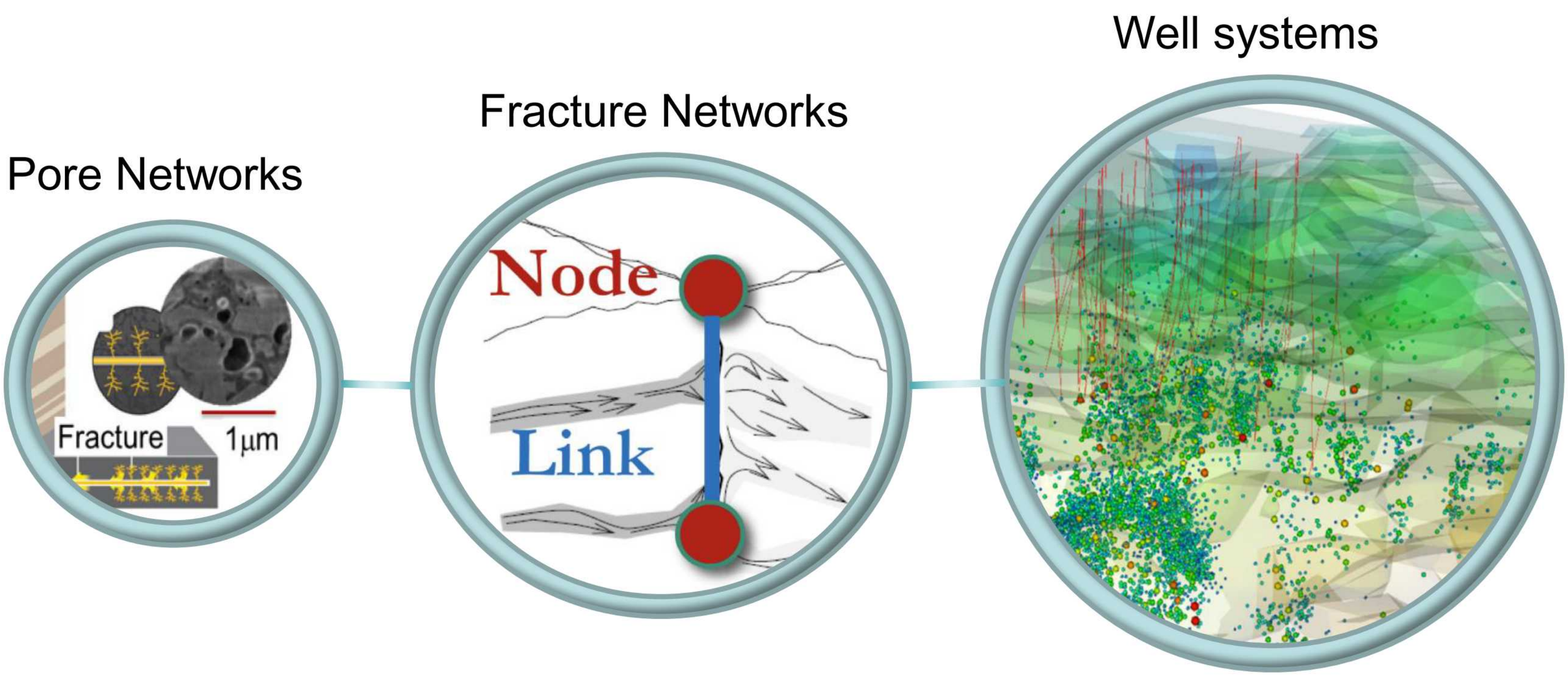

Key Characteristics of Production from Unconventional Reservoirs

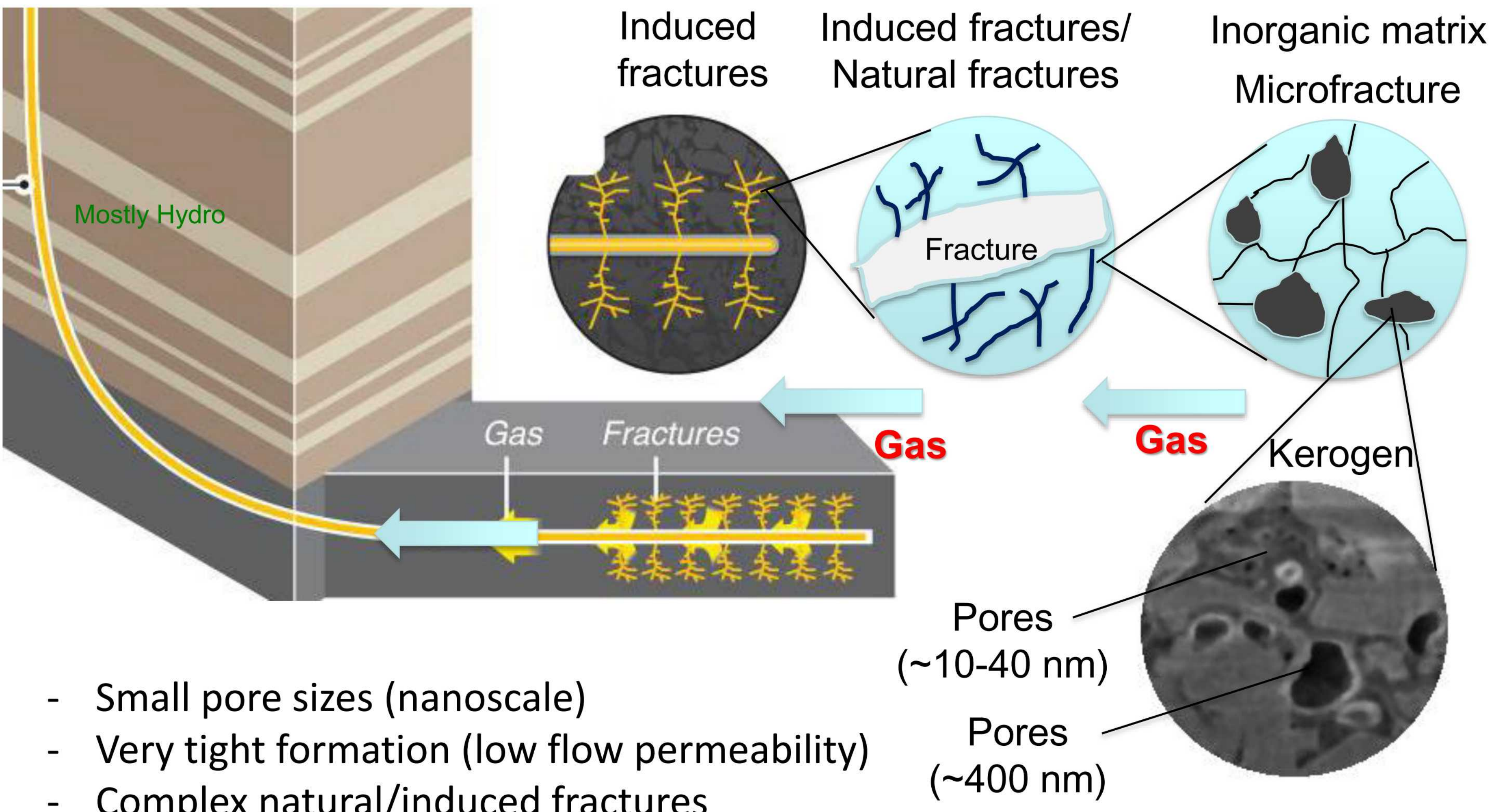

- Small pore sizes (nanoscale)
- Very tight formation (low flow permeability)
- Complex natural/induced fractures

Source: Reuters (National Geographic, Chesapeake Energy, EIA, USGS)

Production Uncertainty

- Gas demand & supplies
- Market prices
- Estimation of total reserves

- Resources recovery limits
- Physical, chemical, mechanical properties
- Hydraulic fracturing efficiency
- Cost reduction

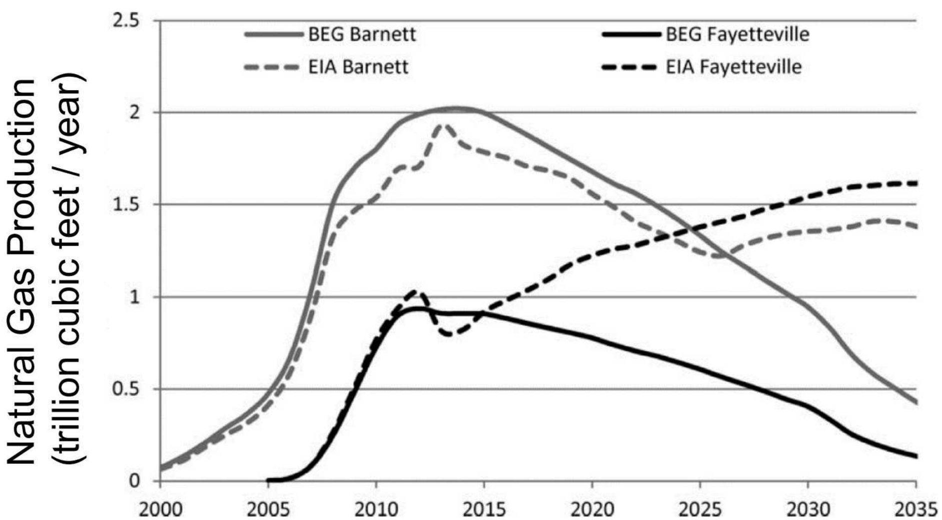

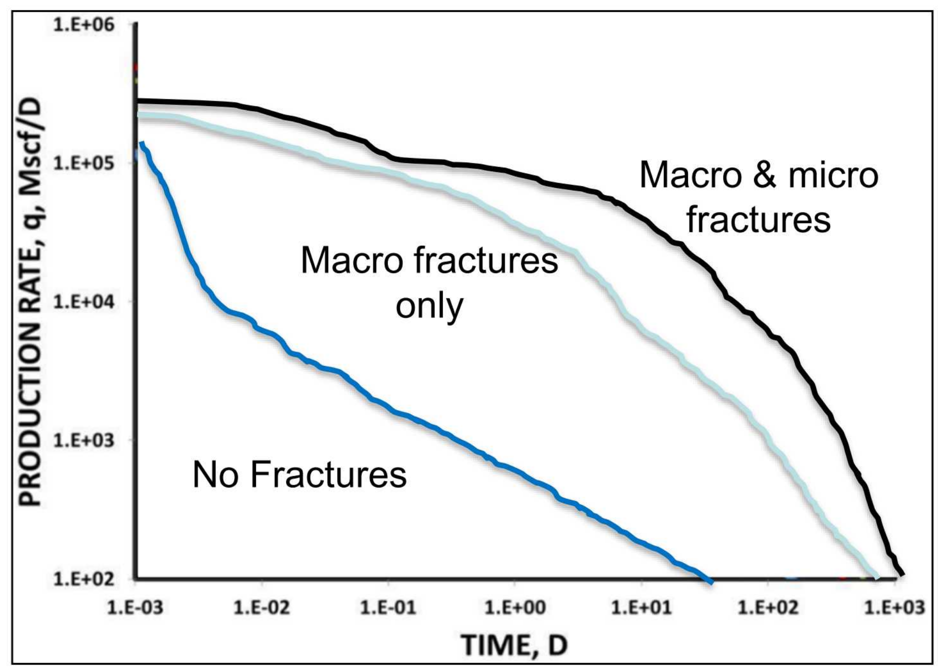

Source: Figure (left) adapted from Ikonnikova S., Browning, J., Gulen, G. Smye, K. and S.W. Tinker, 2014, Factors influencing shale gas production forecasting: Empirical studies of Barnett, Fayetteville, Haynesville, and Marcellus Shale plays, Economics of Energy & Environmental Policy, Vol. 4, No. 1. Figure (right): Apaydin et al. 2011, SPE

Sweet Spot Characteristics

- Well & Frac Stage locations
- Favorable for geochemical, geomechanical and geological parameters

Lithofacies
- Kerogen type, TOC
- Thermal maturity
- Fluid
- Depositional environment

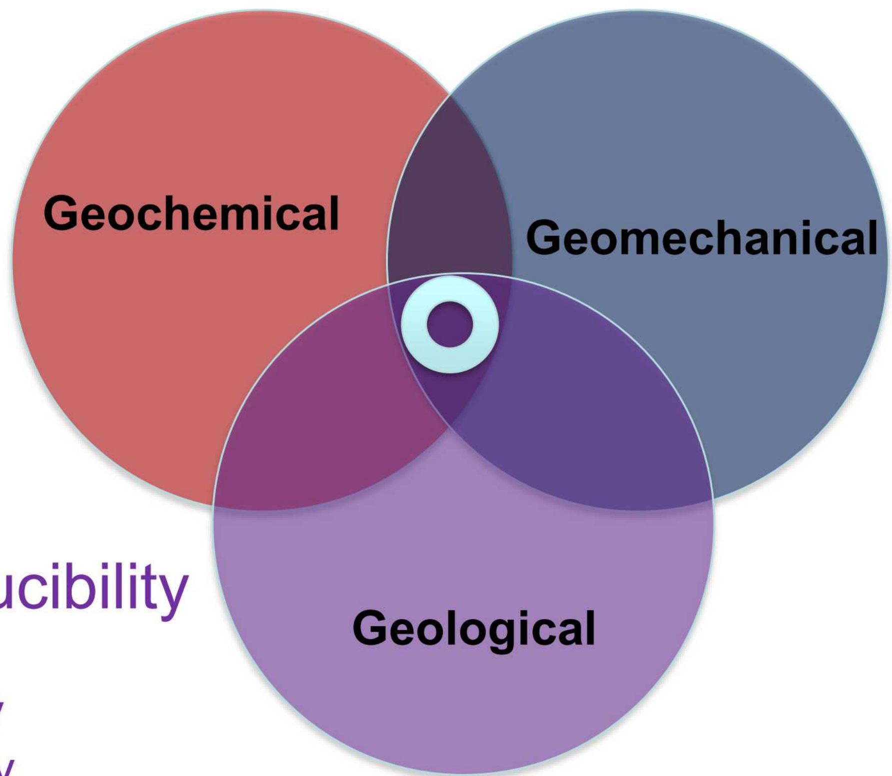

Fracturability
- Anisotropy
- Stress regime
- Fractures/faults
- Brittleness

Continued Producibility
- Depth, thickness
- Lithology/Mineralogy
- Permeability/Porosity
- Pressure

Source: Adapted from Usman Ahmed, 2014, Optimized Shale Resource Development using proper placement of Wells and Hydraulic Fracture Stages, SPE Distinguished Lecture

Avoid Sharp Production Decline

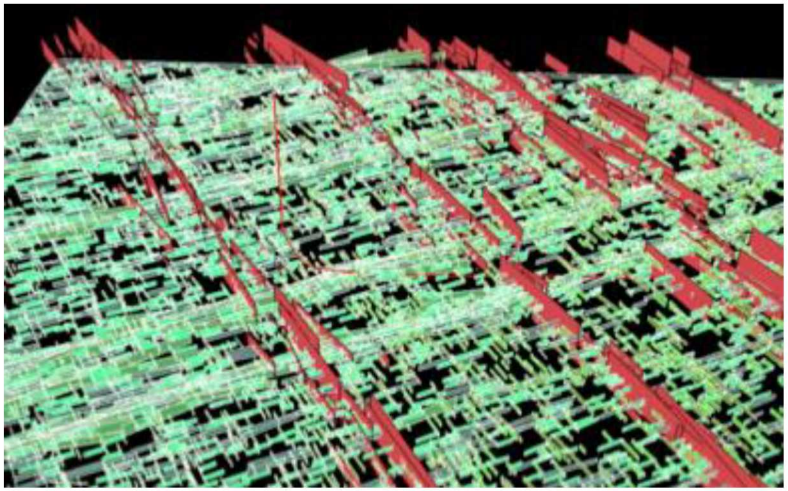

Source: Pointe, ARMA e-newsletter, Spring 2014

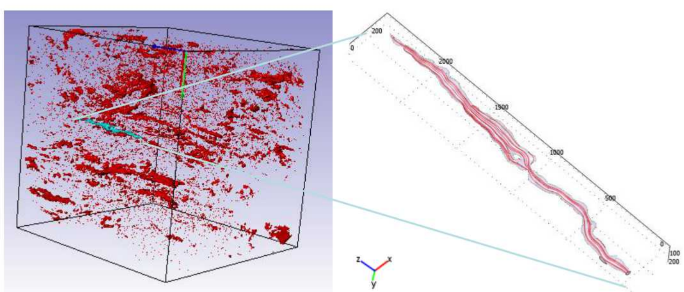

- Discrete fracture network model from the combined geomechanical and geological model
- Reservoir simulation model coupled with flow and transport from nano-Darcy shale rocks
- Development of simulation tools for multiple wells and stages
- Integrated shale science approaches to develop “shale engineering” for economic evaluations

REAL-TIME SUBSURFACE EVENT ASSESSMENT AND DETECTION

Goal: real-time monitoring of changes in the subsurface

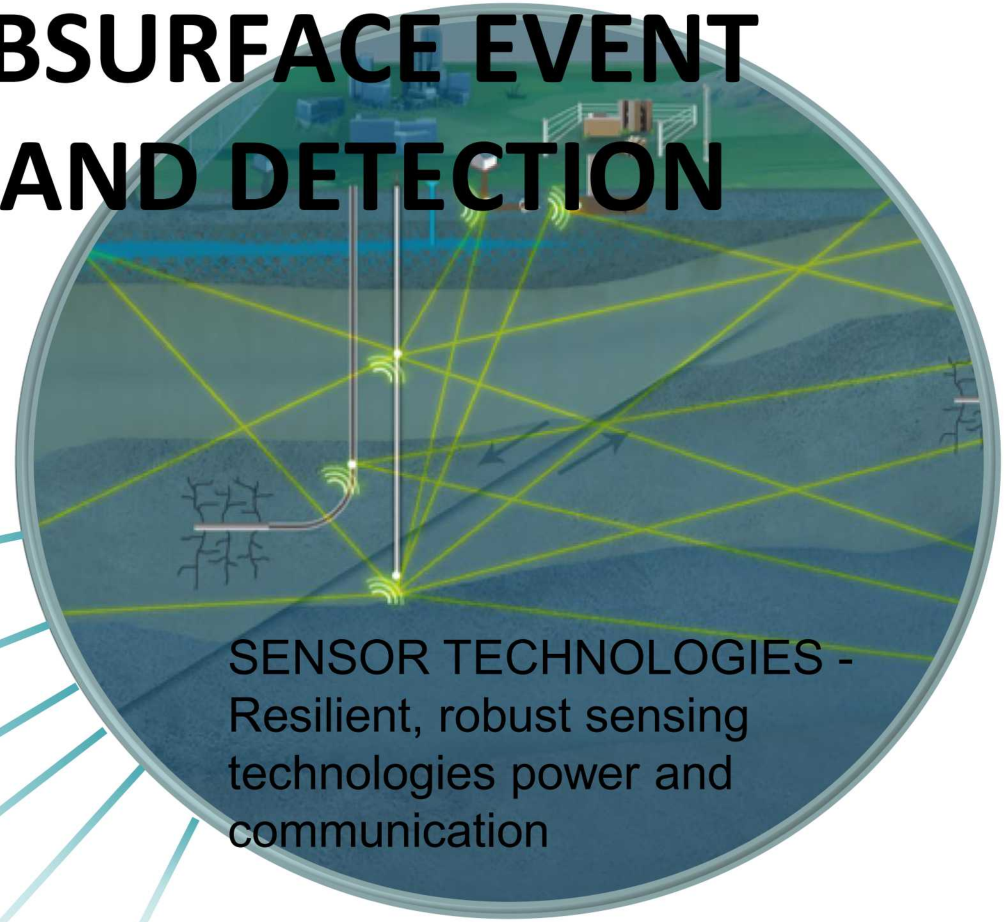

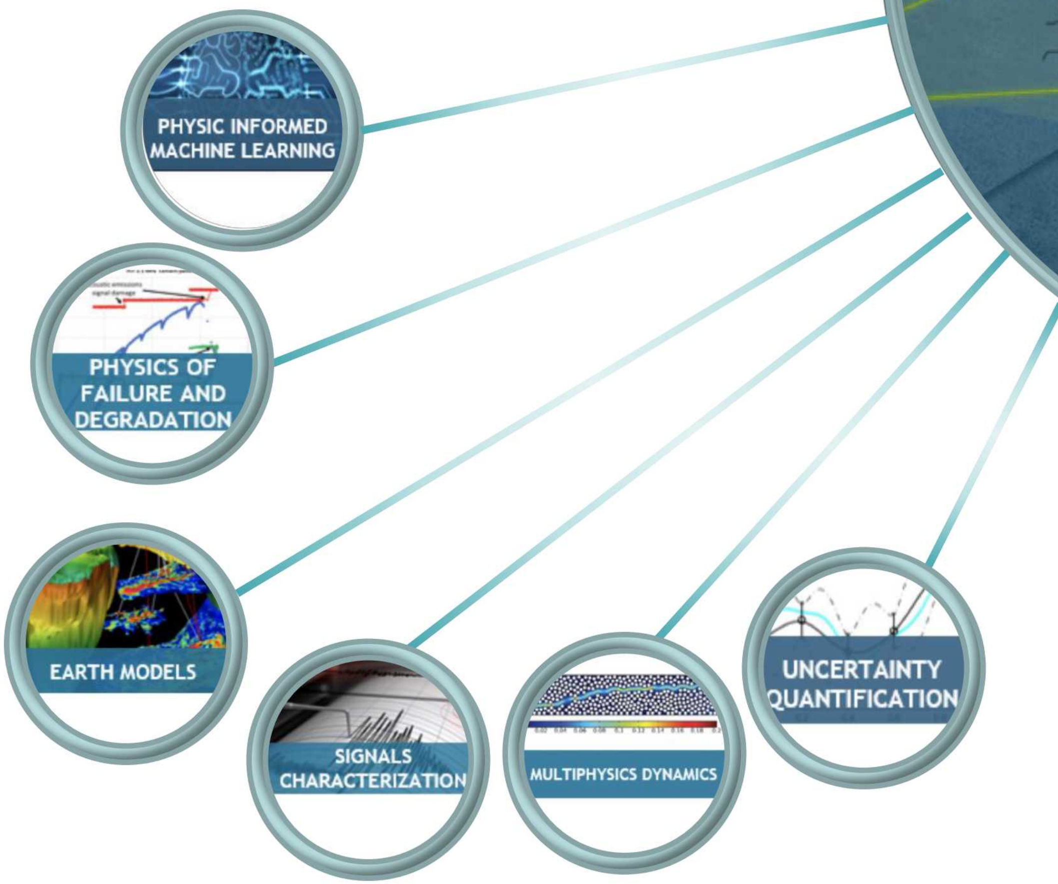

SENSOR TECHNOLOGIES - Resilient, robust sensing technologies power and communication

SOURCE PHYSICS - Comprehensive models of events of interest

DATA SCIENCE - Real-time multi stream signal processing and event flagging

Multiscale network and flows with ROMs + ML

Horn River Shale Gas (CA)

- International collaboration with Korea Gas Corporation (KOGAS)
- Extensive Reservoir characteristics (3D seismic data & microseismic data, well logs (gamma ray, resistivity, sonic, porosity, etc), core sample analysis)
- Integrated 3D reservoir model & geomechanical and geophysical model
- Dynamic production data

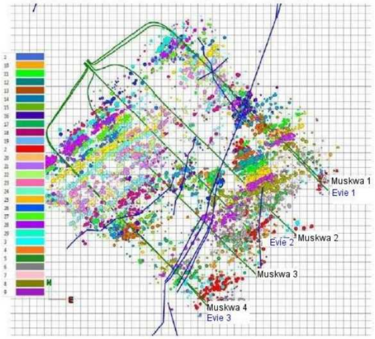

Microseismic data
(courtesy from KOGAS)

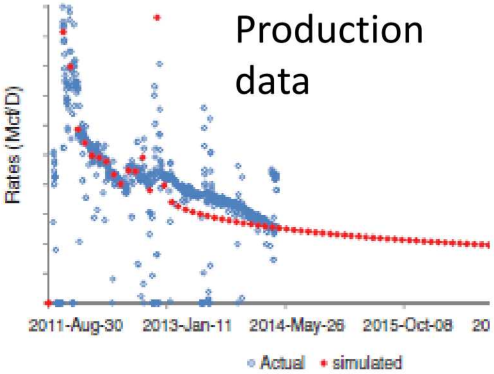

Ref: Kam et al. (2015, SPE-171611-PA)

Summary

- Integrated multiscale imaging and mechanical testing with numerical simulation provides a robust approach to advancing our understanding of shale (poro-) mechanical behaviors
- Texture/mineralogical characterization
  - – Recent advances in mineralogical mapping with high resolution imaging over the large area
  - – Multiscale mineralogical and geologic features lead to considerable heterogeneity of mechanical properties
- Mechanical tests
  - – Macroscopic and microscopic lithofacies have distinctively different mechanical properties
  - – Bulk properties/averaging theory may be misleading as they can represent averages of mechanically heterogeneous rock
  - – Microscopic heterogeneity of mechanical properties can control the spatial distribution of fractures
  - – This heterogeneity should be taken into account for realistic mechanical modeling and can scale up by rigorous theoretical and numerical modeling

Summary

- Advances in production operations, completion, operational design for unconventional shale plays over the past 5 years
- Advances in Data Analysis in quantifying unconventional reservoir characteristics
  - Low porosity & permeability, complex fractures, estimation of stimulated reservoir volume (e.g., microseismic analysis), wide commercial boundary
- A "first principle" approach to unconventional resources has been modestly adopted by industry
  - Flow and production mechanisms from nano-Darcy Shale
  - Physical, chemical, and mechanical properties of rocks
  - Their influence on hydrofracturing propagation
  - Development of robust discrete fractured networks
  - Alternatives to fracking fluids and mitigation of environmental impacts